Journal
International
I J M E
of Modern
Engineering
ISSN: 1930-6628
www.ijme.us

INTERNATIONAL JOURNAL OF MODERN ENGINEERING

Fall/Winter 2008
Volume 9, No. 1

The Leading Journal of Engineering, Applied Science and Technology

Industrial
Electronics
Biomedical
Civil
Aerospace
Computer
Electrical
Chemical
Mechanical

ENGINEERING

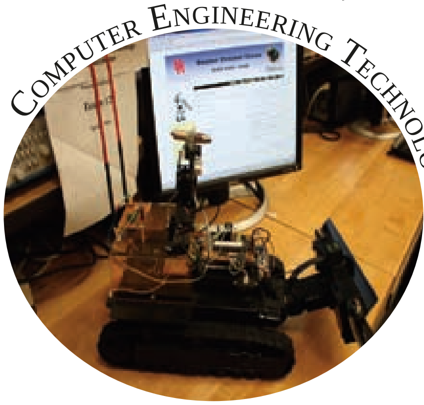

Engineering Technology Opens the Door to a World of Opportunity

We Create Opportunities All Over the World

The University of Houston's College of Technology is leading the future of innovation through the advancements of its Department of Engineering Technology.

- Initiatives including courses in biotechnology and petroleum engineering technology
- In the 2006 ASEE list of 50 schools that offer B.S. degrees in engineering technology, UH ranked 8th in the number of degrees awarded and 5th in the number of degrees awarded to women
- Six state-of-the-art engineering technology research labs including the AT&T Technology Lab
- Exceptional growth in the construction management technology and network communications master's degree programs
- Over $1M in expenditures from external grants and contracts
- Robotics community outreach via Coordination of Robotics Education (CORE)
- Student internships and other opportunities through the Texas Manufacturing Assistance Center (TMAC)
- Over 750 students and 33 faculty and staff

COLLEGE OF TECHNOLOGY
University of Houston

UNIVERSITY OF HOUSTON
Learning. Leading.

www.tech.uh.edu
Engineering Technology / 304 Technology 2 Building / Houston, TX 77204-4021
713-743-4100

INTERNATIONAL JOURNAL OF MODERN ENGINEERING

INTERNATIONAL JOURNAL OF MODERN ENGINEERING (IJME) is an independent and nonprofit publication which aims to provide the engineering community with a resource and forum for scholarly expression and reflection.

IJME is published twice annually (Fall and Spring issues) and includes peer-reviewed articles, book and software reviews, editorials, and commentary that contribute to our understanding of the issues, problems, research associated with the engineering and related fields. The journal encourages the submission of manuscripts from private, public, and academic sectors. The views expressed are those of the authors, and do not necessarily reflect the opinions of the IJME or its editors.

EDITORIAL OFFICE:
Mark Rajai, Ph.D.
Editor-In-Chief
Office: (818) 677-2167
Email: editor@ijme.us
Dept. of Manufacturing Systems
Engineering & Management
California State University
Northridge
18111Nordhoff Street
Northridge, CA 91330-8332

THE INTERNATIONAL JOURNAL OF MODERN ENGINEERING EDITORS

TABLE OF CONTENTS

EDITOR'S NOTE: 2008 IAJC-IJME INTERNATIONAL CONFERENCE

Mark Rajai, IJME Editor and IAJC President

2008 IAJC-IJME International Conference

The 2008 IAJC-IJME International Conference, like the 2006 IJME-Intertech Conference, was a great success. It was sponsored by the International Association of Journals and Conferences (IAJC), which include 14 member journals and numerous universities and organizations.

IAJC is a first-of-its-kind, pioneering organization acting as a global, multilayered umbrella consortium of academic journals, conferences, organizations, and individuals committed to advancing excellence in all aspects of technology-related education.

Conference Statistics

A total of 487 abstracts from more than 150 educational institutions and companies were submitted from around the world. After a multi-level review process—papers were subjected to blind reviews by three or more highly qualified reviewers—a total of 143 papers were accepted and published in the conference proceedings. This reflects an acceptance rate of less than 30%, which is one of the lowest acceptance rates of any international conference. Authors included presidents, deans, chairs, faculty, industry experts, and students representing more than 100 major educational institutions and companies from the United States and 15 other countries.

This conference had three divisions: Engineering (ENG), Engineering Technology (ENT), and Industrial Technology (IT). Selected papers from this conference will be considered for publication in one of the growing list of (currently 14) IAJC member journals.

The 2008 IAJC-IJME International Conference was held at the Music City Sheraton Hotel in Nashville, TN, USA, November 17-19, 2008.

Editorial Changes and IJME New Management

We are pleased to report that Dr. Sohail Anwar of Penn State has returned to resume his former position with the journal. Dr. Anwar was the the journal's Executive Editor since its inception but took some time off to serve as editor-in- chief of the Journal of Engineering Technology. Dr. Li Tan of Purdue University North Central is our new Financial Editor and Copy Co-Editor. Saeed Namyar, of Namyar Solution Inc., is the IJME Web Administrator.

Also, at the annual meeting of the IAJC board of directors held at the site our 2008 conference in Nashville, TN, USA, the board voted unanimously to place the management of IJME under its supervision and to dissolve the IJME board of directors. IJME is now the official and flagship journal of IAJC.

Acknowledgment

Organizing a major conference was a monumental task. I want to thank the conference committee and all division/session chairs and reviewers for their hard work in developing an exciting program. I also want to thank the University of Houston for its continued support and the University of Harford for publishing the hardcopy of this issue.

It is our sincere hope to continue offering such high-quality conferences in the future. To this end, we are seeking dedicated individuals to join us on the planning committee for the next conference. Please look for our advertisement at http://www.IAJC.org.

We hope you enjoy this special issue (dedicated to selected papers from our 2008 conference) and continue to support the journal and its parent organization.

STETHOSCOPE FOR MONITORING NEONATAL ABDOMINAL SOUNDS

Jonathan M. Hill, University of Hartford; Andrew Maloney, University of Hartford; Kelly Stephens, University of Hartford; Ronald S. Adrezin, United States Coast Guard Academy; Leonard Eisenfeld, Connecticut Children's Medical Center

Abstract

This research involves the development of a custom electronic stethoscope system for monitoring abdominal or so-called bowel, sounds in premature infants. Possible causes of bowel dysfunction in premature infants include bowel obstruction, functional or anatomic, which may be reflected as an abnormality or lack of peristalsis. Such dysfunction is problematic to feeding the infant. This peristalsis may be monitored acoustically to determine the health of the patient's digestive tract. Due to the relative lack of research involving infants in this field, we are performing this research in several phases. Starting with our initial research, our current system utilizes a commercial electronic stethoscope.

The second phase is development of a custom electronic stethoscope system appropriate for a bowel sounds monitoring device, for which our preliminary research is being used in the design. Our custom stethoscope will have unique characteristics. The stethoscope will remain attached to the patient for extended periods and, compared to the patient, must be small in size. Unlike an adult, regions in the neonate abdomen are much smaller and may not be acoustically isolated. Also, unlike a conventional device, the stethoscope must be optimized for listening to sounds common in the abdomen. Results from this new stethoscope are compared with other preliminary results that we have obtained and will be used to further characterize bowel sounds in premature infants.

Introduction

The overall goal of our research is to develop an electronic monitoring device for premature infant gastrointestinal sounds detection and analysis. Such a device will continuously present data in a form meaningful to medical personnel and may help diagnose or prevent life threatening problems such as necrotizing enterocolitis, which is an inflammatory disease of the premature. Additionally, vomiting, gastroesophageal reflux, and pulmonary aspiration of gastric contents may be prevented.

Premature infants receive nutrition much earlier in the development cycle than infants with full-term delivery.

Given the situation, the premature digestive system may not be receptive to nutrition, and caretakers must decide whether it is safe to feed the premature infant. Gastrointestinal dysfunction has a number of causes that include immaturity of the digestive tract, birth defects, mild intolerance or allergic reaction to food, enzyme abnormality, electrolyte imbalance, abnormal vascular supply, infection, and systemic illness. Symptomatic of such dysfunction is an abnormality, or lack of peristalsis, which is the pattern of smooth muscle contractions that moves materials through digestion.

Peristalsis may be monitored acoustically to determine the health of the patient's digestive tract. It is currently common practice for nurses to use traditional stethoscopes to periodically listen for and analyze bowel sounds. We assert that gastrointestinal sounds, or so-called bowel sounds, are to be considered among other vital signs. Unfortunately, the ability to identify the aural cues in bowel sounds is a learned skill that takes time to develop. Also, given the sometimes transient nature, some bowel sounds may not be heard. In addition, the interpretation of bowel sounds is currently entirely subjective and based on training and experience. Further, the human ear is limited in its sensitivity and specificity in detecting bowel sounds. Based on these reasons, clinical acumen is limited, and such findings may or may not be correct.

The goal of this specific project is to develop a specialty stethoscope designed for recording the bowel sounds of premature infants. Due to the relative lack of research in this field, we are performing this research in several phases. Our initial research utilizes an FDA approved commercial electronic stethoscope and is part of a clinical study at the Connecticut Children's Medical Center [1]. Based on this research, we are developing a new prototype stethoscope system. Results from this new stethoscope will be compared with other preliminary results that we have obtained and will be used to further characterize bowel sounds in premature infants.

Related Research

Relevant references include Tomomasa, et al. [2], who recorded and analyzed bowel sounds of infants with pyloric stenosis, before and after applying a corrective pyloromyotomy. According to Wikipedia [3], infantile hypertrophic pyloric stenosis is a condition whereby an obstruction in the lower stomach causes severe vomiting in the first few months of life. Few cases are mild enough to be treated medically. The definitive treatment is with a surgical pyloromyotomy, known as Ramstedt's procedure, which involves dividing the muscle that narrows the pylorus. Occasionally, the procedure must be repeated to provide an adequate opening.

To record bowel sounds, the study used methods previously reported by Tomomasa et al. [4], [5] whereby a handmade device using a condenser microphone was attached with electrocardiograph adhesive tape to the abdomen. Signals were amplified and recorded with an audio cassette deck over periods each 60 minutes long when fasted. The analog recordings were later sampled and analyzed using a personal computer. Following an 80 Hz high-pass filter to suppress cardiovascular sounds present in the 20 to 50 Hz range, sampling was performed at 1,000 Hz. Three-minute bins were used to calculate the sound index (SI) as the sum of absolute signal amplitudes expressed as volts per minute.

The results show that bowel sounds increased after pyloromyotomy, correlating with gastric emptying, except for the first 24 hours when gastric emptying reached the plateau level. They cite Benson et al. [6] who demonstrated by manometry that small intestinal motility was abnormal after major abdominal surgery. Bowel sounds were also monitored by stethoscope and were found to be absent from subjects for more than 20 hours. Approximately 60 hours were required for bowel sounds to return in 50 percent of the subjects. To summarize, bowel sounds are a good indicator of the return of gastric emptying, as well as bowel motility after pyloromyotomy and can be useful in deciding when to resume feeding post-operatively in each patient.

With respect to the interests of this paper, Dimoulas et al. [7] provide a useful survey of additional relevant research. They cite the pioneering work of Cannon [8] and others. Issues in recording bowel sounds involving noise, dynamic range, and pickup are outlined. Cardiac and respiratory acoustic interference has been reported where the heartbeat sounds have a very weak nature and are observed mostly in the cases of infants. Patterns of bowel sounds are defined and classified. Data was sampled at a rate of 8 kHz and was found to be entirely adequate. A 16-bit quantization was selected to provide adequate dynamic range.

Initial Research

Figure 1 shows the stethoscope configuration used in our initial research, which is based on a commercially available electronic stethoscope [9] and acquisition module [10] that connects to a laptop computer (not shown) for data collection. The black box contains a custom amplifier used to better condition the stethoscope signal to the acquisition module. Like conventional devices, this stethoscope includes earpieces that are placed in the listener's ear canal, ear tubes that are solid material fitted to the ear pieces, tubing, as well as a chest piece, or stethoscope head, that is placed against the region of interest. Reference to the head as a pickup is suggestive of electro-mechanics, like that in an electronic stethoscope.

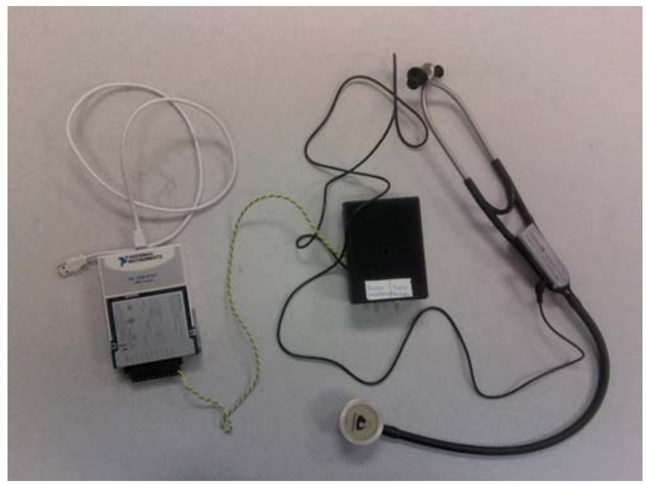

Figure 1. Initial Research Configuration with Commercial Devices

The initial research configuration is approved by our Institutional Review Board (IRB), which allows us to actually use the device in the Neonatal Intensive Care Unit (NICU). The IRB analysis was eased greatly since the Thinklabs stethoscope is an FDA approved device. Bowel sounds were recorded in a number of situations, such as before and after feeding. Figure 2 shows bowel sounds from a normal premature infant, less than two months in chronological age, recorded before feeding. To an untrained ear, such a recording sounds like popping at first. While limited and not satisfying our design goal, this configuration has helped us to understand the nature of infant bowel sounds.

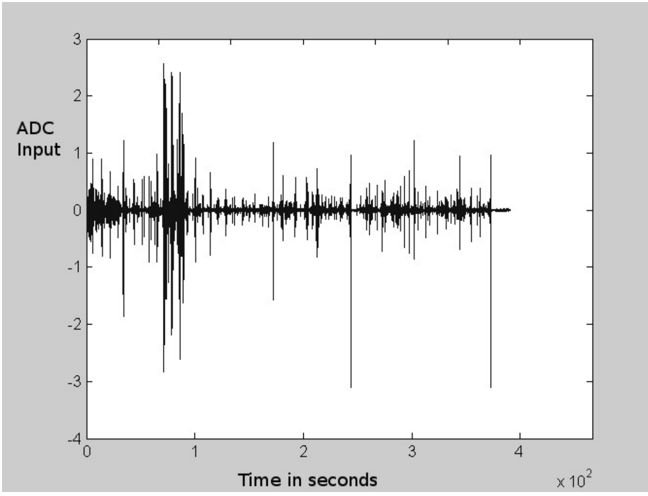

Figure 2. Normal Premature Infant Bowel Sounds before Feeding

To understand how this configuration is limited for our use, consider that the stethoscope head is somewhat large and heavy. A feature to extend battery life limits use of the stethoscope to approximately two-minute intervals. Such a stethoscope is for general use and, for our specific application, may introduce selective distortion. The stethoscope must be carefully held against a patient, which introduces undesirable acoustic artifacts.

Our initial research is being used to design a custom stethoscope system, specifically for such a bowel sound monitor. The stethoscope has unique characteristics. Eventually, such a stethoscope will remain attached to the patient for extended periods and, compared to the patient, will be small in size. Unlike an adult, regions in the infant abdomen may not be acoustically isolated. Also, unlike a conventional device, the stethoscope must be optimized for listening to sounds common in the abdomen. Following our IRB approval, results from this new stethoscope will be compared with other results that we have obtained and will be used to further characterize bowel sounds in premature infants.

Prototype Stethoscope Concept

Figure **3** summarizes our prototype stethoscope system. The stethoscope head, or pickup, to the left is constructed with a contact mechanism that is in physical contact with the patient, as well as a transducer, which converts the resultant mechanical signal to an electrical signal. The acquisition card contains amplifiers, anti-aliasing filters, and an analog to digital converter (ADC) used to sample and digitize the transducer signal. An off-the-shelf development board [12] contains a field programmable gate array (FPGA) used to implement the processor system. We are first using a laptop computer for data collection, but a compact flash device will allow for long-term stand-alone data collection capability.

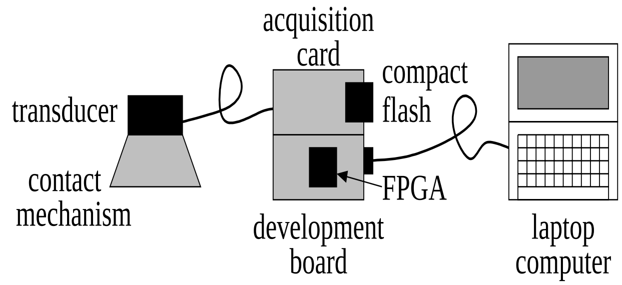

Figure 3. Prototype Stethoscope System

The acquisition card is a custom design made with discrete components. Such use of an FPGA to construct the embedded microprocessor system is appealing because, in prototyping, we benefit in having the utmost in flexibility. Significant changes can be quickly made to the corresponding embedded processor system without incurring any tooling charges. Future research may also involve the use of wireless technology.

The pickup is the most critical component in the design. To be acceptable for use with premature infants, the device must be small but still have a reasonably large contact area, have very little nominal contact pressure, little weight, and maximum sensitivity to the desired signal. To date, our research has produced the two prototype pickup devices in Figure **4**. The devices have similar construction to those described previously, having a contact mechanism and a transducer. The device to the left is a small tube container with an electret microphone and is sealed with thin plastic sheet material. To the right is a conventional stethoscope head that has been bored-out and contains an electret microphone. While the tube contact area is slightly smaller, our first impression of the measurements is that it compares more favorably to the bored-out stethoscope head.

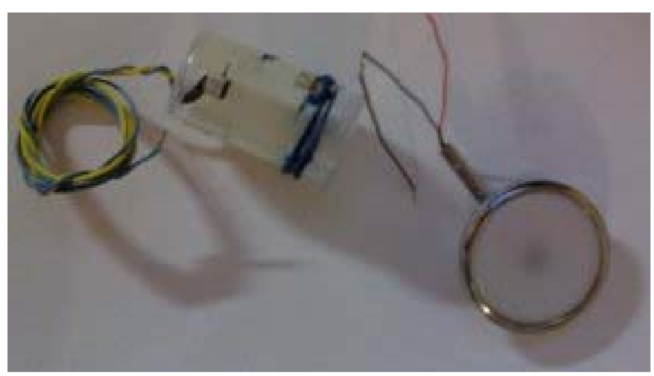
Figure 4. Experimental Pickups

Several other devices were also briefly tried. Piezoelectric elements were more sensitive to the mechanical aspect of being mounted rather than to the desired signal. Dynamic speakers were not very sensitive. The commercial contact devices considered applied too much contact pressure. To allow for long-term patient contact, yet prevent injury to infant skin, an acceptable device may incorporate a specialty adhesive, similar to that currently used for ECG leads and thermal reflective patches. Klear-Trace© brand electrodes [11] are such examples. Future work will refine the contact mechanism and will consider such a specialty adhesive.

Acquisition Card and System Board

Figure 5 shows the prototype stethoscope system with the tube type pickup attached using test leads. The acquisition card is in the upper right, with a Compact Flash (CF) card to the far right. The lower card is an off-the-shelf development board [12] used to implement the digital aspects of the design. This prototype stethoscope currently does not actually have a headphone connector for direct listening because we presently rely on an attached personal computer to examine the incoming signals. Providing such a headphone connector makes the stethoscope more usable as a standalone system.

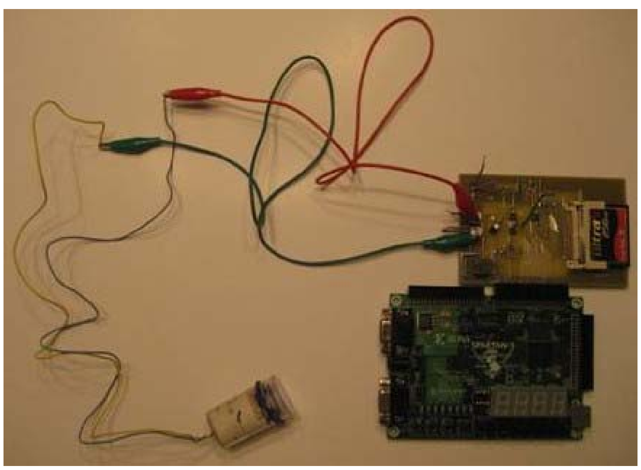

Figure 5. Prototype System with the Tube Pickup

The availability of low-cost, high density field programmable gate arrays (FPGAs) provides new opportunities for the development of small embedded processor systems. Figure 6 outlines how the prototype stethoscope contains such a system. A processor is needed to provide all the required behavior, which includes managing a data acquisition system, communicating with other devices, and performing data logging. Also, having the stethoscope implemented as an embedded microprocessor system will enable us to consider advanced algorithms such as those used to mitigate or remove interfering noise.

Much of the system is in the FPGA, which is an array of configurable logic blocks along with a configurable interconnecting resource that is called the FPGA fabric. Such FPGA-based systems are most appropriate in low volume applications that call for the utmost flexibility. Given the modest performance requirements and that development of the stethoscope is only one step in our research, the initial research use of FPGA technology is particularly appealing.

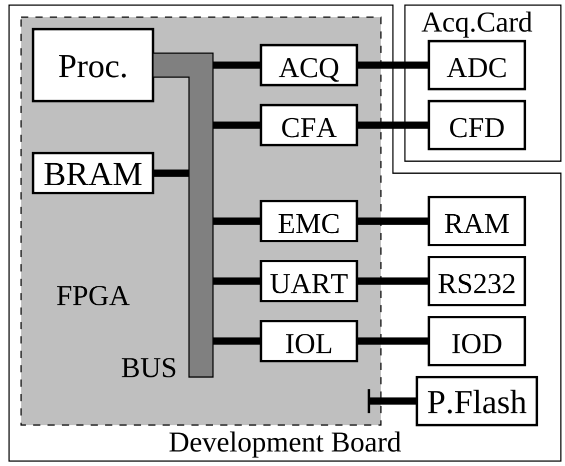

Figure 6. Stethoscope Embedded Processor System

With modest performance requirements, we chose to use a fairly generic 32-bit RISC type soft core microprocessor [13], which means that rather than being an embedded core, the processor (Proc.) is implemented in the fabric along with the rest of the system. Code written with a hardware description language, such as VHDL, is used to produce an image file or bit file, stored in the platform flash (P.Flash), which configures all aspects of the FPGA, including the on-chip block RAM (BRAM) memory. Note that the image file here is not executable but rather can be thought of as being the system itself. Once the FPGA is configured, the system executes machine code just like any processor. As such, the software is written in C using conventional software development tools.

The acquisition card (Acq.Card) contains acquisition components (ADC), which are controlled by the acquisition logic (ACQ). Likewise, a compact flash device (CFD) is controlled by compact flash adapter logic (CFA). On the development board, the external memory controller (EMC) provides access to 1 Mbyte of RAM. A UART provides RS232 communications. Input-output logic (IOL) connects input-output devices (IOD), such as switches, push-buttons, and LEDs and the seven segment display.

For sampling, we selected the AD7685 which provides 16-bit samples at rates as high as 250 kHz. Sample rates are presently limited by the data rate of the associated communications. To further address the issue of large dynamic range inherent with bowel sounds as described by Dimoulas et al. [7], we include digitally controlled potentiometers to maximize the dynamic range of the sampler. Input configurations are provided for differential, as well as single ended, signal sources.

Given that the required IRB analysis of the prototype system is not completed, we are not yet able to use the system to actually record premature infant bowel sounds. Unlike our Thinklabs stethoscope-based system, the prototype system is not FDA approved and requires a more rigorous study. To prepare for examining the prototype system, we first considered heartbeat sounds. Figure 7 is a sample published recording of an adult heartbeat sound [11] sampled at 44.1 kHz that was dynamically enhanced.

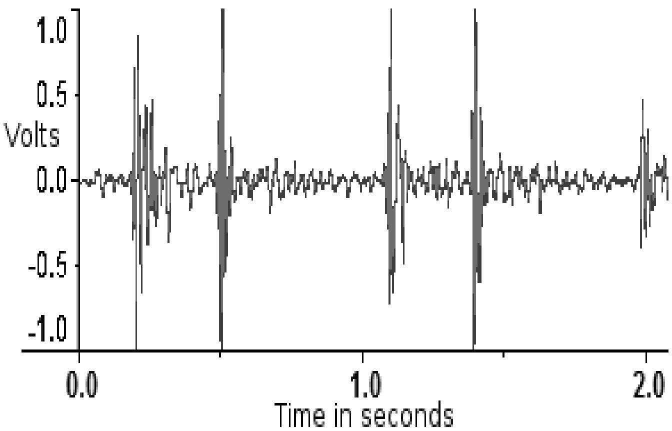

Figure 7. Adult Heartbeat Sound

Figure 8 and Figure 9 are among the first results we produced with the prototype stethoscope system. As a first test, we recorded Andrew Maloney's heartbeat; Maloney is one of our participating graduate students. Figure 8 shows the analog signal of a pair of beats before sampling. Figure 9 presents the corresponding digital output of a single beat plotted by LabVIEW [14]. In this test, the sample rate is 3,000 Hz. Results from the Thinklabs' electronic stethoscope and our prototype compared over an extended period of time appear very similar.

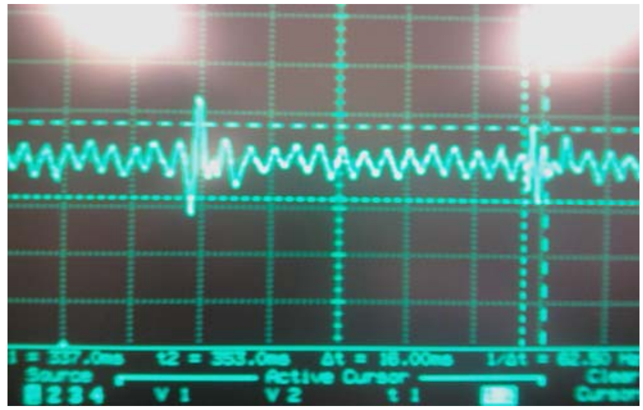

Figure 8. Analog Input to Sampler of Adult Heartbeat

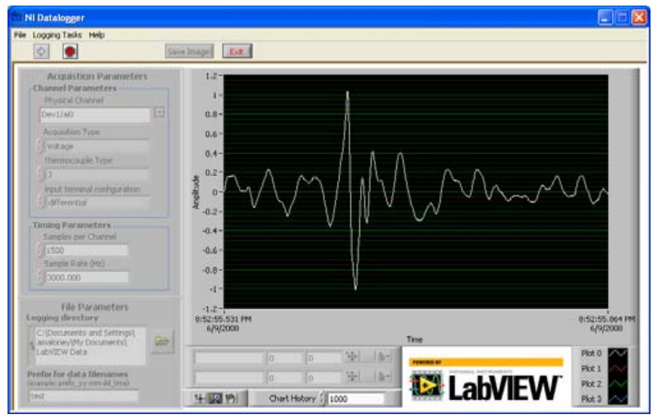

Figure 9. First Digital Results from Prototype of Adult Heartbeat

Figure 10, displayed in MATLAB, shows bowel sounds from our graduate student produced by the prototype stethoscope using the bored-out stethoscope head. In comparing this to Figure 2, taken of a premature infant with the initial research configuration, they share a similar pattern of peaks although they are different. The amplification and anti-alias filtering used to obtain Figure 10 does not eliminate the considerable background noise.

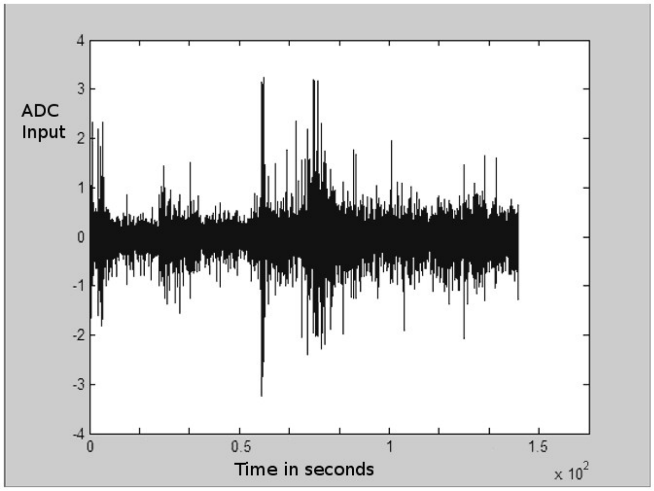

Figure 10. Prototype Recording of Adult Bowel Sounds

Next Research Phases

The first issue, with respect to the prototype stethoscope system, is obtaining approval from our IRB to allow us to use the device in the NICU. We are also planning the next generation prototype stethoscope, on which we will use a next generation stethoscope head. Through interviews with one of our authors, Dr. Eisenfeld, along with attending nurses, students produced a Quality Function Deployment (QFD) report. Such a report is based on a short list of questions first posed to the perceived customers of a proposed product. Results from the list are used to inspire a second list of questions. A summary of the final results serves as useful input to the product design cycle. The most important elements identified were computer control, weight, the ability to capture, filter, and amplify all bowel sounds without signal loss, as well as compatibility with other existing hardware in the NICU.

Summary

In closing, the subject of this paper is the development of a custom electronic stethoscope system for monitoring abdominal or so-called bowel sounds in premature infants. This research is part of a larger project to design a system for monitoring and evaluating bowel sounds. This paper outlines initial research being performed, based on an FDA approved stethoscope. This research has led to the design of a unique prototype stethoscope for use in this regard. We are seeking approval from our IRB to allow us to use the device in the NICU. Listening to adult bowel sounds is a necessary first step in our research toward developing such a monitor system. We are also planning the next generation prototype stethoscope. Work in the larger project will involve practical analysis and classification of such recordings. Situations that involve comparing bowel sounds before and after eating will be considered. This is based on the premise that bowel sounds are notably more pronounced before eating because the muscles of the stomach and intestines are active before digestion.

References

[1] J. Hill, M. Regan, R. Adrezin, and L. Eisenfeld, "System for Recording the Bowel Sounds of Premature Infants," ASME Biomed 2008 Conference, June 2008.

[2] Takeshi Tomomasa, MD, Atsushi Takahashi, MD, Yasushi Nako, MD, Hiroaki Kaneko, MD, Masahiko Tabata, MD, Yoshiaki Tsuchida, MD, and Akihiro Morikawa, MD, Analysis of Gastrointestinal Sounds in Infants With Pyloric Stenosis Before and After Pyloromyotomy, *PEDIATRICS*, Vol. 104 No. 5 November 1999, p. e60, http://pediatrics.aappublications.org/ cgi/content/full/104/5/e60.

[3] Wikipedia, Pyloric Stenosis, http://en.wikipedia.org/ wiki/Pyloric_stenosis, retrieved June 15, 2008.

[4] Tomomasa T, Morikawa A, Tabata M, Hyman PE, Itoh Z, "Bowel Sounds Reflect Gastrointestinal Motility and Small Intestinal Transit Time in Fasted Humans," *Gastroenterology,* 1997, 112:839.

[5] Tomomasa T, Morikawa A, Sandler RH, "Gastrointestinal Sounds and Migrating Motor Complex in Fasted Humans," *Am J Gastroenterol,* 1999, 94:374–381.

[6] Benson MJ, Roberts JP, Wingate DL, "Small Bowel Motility Following Major Intra-abdominal Surgery: the Effects of Opiates and Rectal Cisapride," *Gastroenterology,* 1994, 106:924–936.

[7] C. Dimoulas, G. Kalliris, G. Papanikolaou, V. Petridis, A. Kalampakas, "Bowel-sound Pattern Analysis Using Wavelets and Neural Networks with Application to Long-term, Unsupervised, Gastrointestinal Motility Monitoring," *Expert Systems with Applications*, Volume 34, Issue 1, January 2008, pp. 26–41.

[8] W.B. Cannon, "Auscultation of the Rhythmic Sounds Produced by the Stomach and Intestine," *American Journal of Physiology*, 1905, 13, pp.339–353.

[9] Thinklabs, ds32a Stethoscope, http://www.thinklabsmedical.com/.

[10] National Instruments, http://www.ni.com/.

[11] Klear-Trace© brand, CASMED, http://www.casmed.com/kleartrace.html.

[12] Spartan-3 Starter board, http://www.digilentinc.com.

[13] Spartan-3 and Microblaze Documentation, http://www.xilinx.com.

[14] National Instruments LabVIEW, http://www.ni.com/labview/.

[15] A. Karivaradhan, C. Diyaolu, K. Stephens, Analysis and Interpretation of Infant Gastrointestinal Sounds, *University of Hartford Senior Design Report*, December 14, 2007, unpublished.
[16] Recording of Herbert Boland's heartbeat, HeartbeatEnhanced.wav, copyright March 25, 2007, Creative Commons License, http://www.freesound.org/.

Biographies

JONATHAN HILL *(all caps for author's name)* is an assistant professor in Electrical and Computer Engineering at the University of Hartford in Connecticut. He instructs graduate and undergraduate computer engineering computer courses, directs graduate research, and performs research involving embedded microprocessor based systems. Specific projects involve digital communications, signal processing, and intelligent instrumentation. Dr. Hill may be reached at jmhill@hartford.edu

ANDY MALONEY is a graduate student in Electrical and Computer Engineering in the College of Engineering, Technology, and Architecture (CETA) at the University of Hartford in Connecticut. He received a bachelor's degree in Electrical Engineering from the University of Hartford. His interests involve analog and digital electronics, as well as computers. Mr. Maloney may be reached at amaloney@hartford.edu

KELLY STEPHENS is a graduate student in Mechanical Engineering in the College of Engineering, Technology, and Architecture (CETA) at the University of Hartford in Connecticut. She received a bachelor's degree in Biomedical Engineering from the University of Hartford. Her interests involve research into human biomechanics in orthopedic surgery, as well as bioinstrumentation and biomaterials as they relate to diagnosis and treatment of animals. Ms. Stephens may be reached at kstephens@hartford.edu.

RONALD ADREZIN, P.E., is an Associate Professor in Mechanical Engineering at the United States Coast Guard Academy. He also serves as the Executive Director of the Center for Life Support and Sustainable Living. He was previously an engineer in industry, working with institutions that include the National Institutes of Health. His interests include design and dynamics applied to aerospace and medical applications. Professor Adrezin may be reached at ronald.s.adrezin@uscga.edu

LEONARD EISENFELD, M.D., is an attending neonatologist at the Neonatal Intensive Care Unit (NICU) of Connecticut Children's Medical Center. He is an Associate Professor of Pediatrics and an Adjunct Associate Professor of Biomedical Engineering at the University of Connecticut. His interests include neonatal biomedical device conception and development. Dr. Eisenfeld may be reached at leisenf@ccmckids.org

DETERMINING MACHINING PARAMETERS OF CORN BYPRODUCT FILLED PLASTICS

Kurt A. Rosentrater, United States Department of Agriculture – Agricultural Research Service;
Andrew W. Otieno, Northern Illinois University; Pratyusha Melampati, Northern Illinois University

Abstract

In a collaborative project between the USDA and Northern Illinois University, the use of corn ethanol processing byproducts (i.e., DDGS) as bio-filler materials in the compression molding of phenolic plastics has been studied. This paper reports on the results of a machinability study in the milling of various grades of this material. Three types of samples were studied: 100% (0% DDGS), 75% (25% DDGS), and 50% (50% DDGS) phenolic samples. The milling operation was carried out with a fixed depth of cut of 2.0 mm using a 12.5 mm diameter two-fluted end-mill. The cutting speed was varied between 120 and 160 m/min at feed rates between 200 and 300 mm/min. Surface roughness measurements were taken after each combination of feed and speed. Mathematical models for surface roughness have been developed in terms of speed and feed at constant depth of cut by response surface methodology (RSM); the significance of the speed and feed on the surface roughness has been established with Analysis of Variance (ANOVA) for all three types of samples. The optimum cutting conditions were obtained by constructing contours of constant surface roughness using MINITAB statistical software.

Introduction

Plastics are manufactured from petroleum resources, which are not renewable and not biodegradable. To minimize the environmental impact of plastic materials and enhance biodegradability, many plastic products are beginning to utilize low-cost, bio-based materials as fillers. Corn processing coproducts (i.e., DDGS), once dried, represent one such potential biofiller [1]. This filler can be added in a concentration by weight so as to maintain the mechanical and physical properties of the resin. It appears that filler concentrations between 25% and 50% represent reasonable inclusion values and produce sufficient mechanical strength [1]. The aim of this work is to further study these composites by examining the machinability of corn processing coproduct filled plastics.

For the selection of optimum machining conditions Computer Aided Manufacturing (CAM) has been widely implemented. In the present work, experimental studies have been conducted to see the effect of cutting conditions on the machining performance of resin and corn coproduct filled resin composites. This paper presents an approach to develop mathematical models for surface roughness by response surface methodology (RSM) in order to optimize the surface finish of the machined surface [2, 3]. RSM is a combination of mathematical and statistical techniques used in an empirical study of relationships and optimization, where several independent variables influence the process. First and second order mathematical models, in terms of machining parameters, were developed for surface roughness prediction using RSM on the basis of experimental results.

The influence of the speed and feed on the surface roughness has been established with Analysis of Variance for 100% phenolic,75% phenolic (25% DDGS), 50% phenolic (50% DDGS) samples. The response, or dependent variable, was viewed as a surface to which mathematical models were fitted. The optimum cutting condition was obtained by constructing contours of constant surface roughness by MINITAB, and then used for determining the optimum cutting conditions for a required surface roughness.

Methodology

General Approach: Response surface methodology is an optimization technique in the field of numerical analysis. To achieve optimization, it uses a function called a response surface. A response surface is a function that approximates a problem with design variables and state quantities, using experimental results. In general, design of experiments is used for analysis and experiment point parameter settings, and the least squares method is used for function approximation. Response surface methodology is a combination of mathematical and statistical techniques useful for modeling and analyzing problems in which several independent variables influence a dependent variable (i.e., response).

The RSM technique attains convergence by repeating numerical and sensitivity analyses until an optimal solution is obtained, and it is especially good for difficult problems. For example, problems with high non-linearity, and for multimodal problems, there may be cases in which no solution can be found because of inability to obtain sensitivities or a lapse into a local solution. To solve such problems, RSM has often been adopted. With RSM, optimization conditions are first set, and then a response surface is created between design variables and objective functions or constraint conditions [4]. Since the expected experimental and theoretical relations in machining are expected to be non-linear, in this work response surface models were used for optimization.

The mathematical model generally used is represented by:

$$Y = f(v, f, \alpha, r) + \in \quad (1)$$

where Y is the machining surface response, v, f, α, and r are milling variables, and $\in$ is the error (which is assumed to be normally distributed) about the observed response Y with zero mean.

Considering only the parameters v (speed) and f (feed rate), a relation can be formulated between these independent variables and the dependent variable, surface roughness (R_a), as follows [5]:

$$R_a = Cv^a f^b \quad (2)$$

where C is an empirical constant, v is cutting speed (m/min), f is the feed rate (mm/min), and a and b are the empirically-determined exponents.

This mathematical model can be linearized by performing a logarithmic transformation as follows:

$$\ln R_a = \ln C + a \ln v + b \ln f \quad (3)$$

The constants and exponents C, a, and b can be determined by the method of least squares. The first order linear model, developed from the above functional relationship using the least squares method, can be represented as follows:

$$Y_1 = Y - \in = b_0 x_0 + b_1 x_1 + b_2 x_2 \quad (4)$$

where Y_1 is the estimated response. Based on the first-order equation, Y is the measured surface roughness on a logarithmic scale, x_0(=1) is a dummy variable; x_1 and x_2 are logarithmic transformations of cutting speed and feed; b_0, b_1 and b_2 are coefficients found from least squares.

The second order model can then be extended from the first order model's equation as:

$$Y - \in = b_0 x_0 + b_1 x_1 + b_2 x_2 + b_{11} x_1^2 + b_{22} x_2^2 + b_{12} x_1 x_2 \quad (5)$$

And the same method is used to determine coefficients b_0, b_1, b_2, b_{11}, b_{22} and b_{12}.

Experimental Details: Based upon the research conducted by Alauddin et al. [5], which identified feed rate and cutting speed as key variables, in our study a milling operation was performed on each test specimen using different feeds and speeds. Samples were compression molded following [1]. A CNC milling machine was then used to machine a slot using a 12.5 mm diameter carbide two-flute end mill. Six slots were machined on each sample (three on each side). A new end mill was used after every specimen to reduce effects of tool wear on the measured parameters. The depth of cut was kept constant at 2 mm. Table 1 below shows the selected cutting conditions.

The design of experiments used in this study was based on the Taguchi approach [6]. Two factors considered; the range of values for each factor was set at three different levels; all treatments were determined using a full factorial approach. Therefore the total number of tests conducted was 9 (3^2). Table 2 shows the full experimental schedule.

Table 1. The Two Process Variables used in the Experiment were Each at Three Levels

Parameter	Level-1	Level-2	Level-3
Speed, v (m/min)	120	140	160
Feed, f (mm/min)	203	254	305

Table 2. The Experiments were Conducted Following a 3^2 Factorial Design

Experimental Treatment	Speed v (m/min)	Feed f (mm/min)
1	120	203
2	120	254
3	120	305
4	140	203
5	140	254
6	140	305
7	160	203
8	160	254
9	160	305

Coding of Independent Variables: Prior to data analysis, the variables were coded taking into account the capacity and limiting cutting conditions of the milling machine so as to avoid vibration of the work-tool system. The coded values of the variables shown in Table 2 for use in equations (4) and (5) were obtained from the following transformation equations [7]:

$$x_1 = \frac{\ln v - \ln 140}{\ln 140 - \ln 120} \quad (6)$$

$$x_2 = \frac{\ln f - \ln 254}{\ln 254 - \ln 203} \quad (7)$$

where x_1 is the coded value of the cutting speed corresponding to its actual value v, x_2 is the coded value of the feed corresponding to its actual value f. The axial depth of cut, d, was kept constant at 2 mm throughout the study.

Statistical Analysis: Analysis of the Variance (ANOVA) was performed to determine the accuracy of the fit for the response surface models. The ANOVA method is based on a least squares approach. This analysis was carried out using a level of significance (α) of 5% (i.e., a level of confidence of 95%) [8]. The regression parameters of the postulated models were estimated by the method of least squares using the following basic formula [9]:

$$b = (X^T X)^{-1} X^T Y \tag{8}$$

where b is the matrix of parameter estimates, X is the matrix of independent variables, X^T is the transpose of the matrix X, and Y is the matrix of logarithms of the measured surface roughness values (i.e., responses).

Results and Discussion

The variation of machining response with respect to the independent variables is shown graphically in Figures 1 through 3. The graphs show results for 100% phenolic, 75% phenolic and 50% phenolic samples. 100% phenolic samples show minimum surface roughness values at high speeds and low feeds (Figure 1). 75% phenolic samples show minimum surface roughness values at medium speeds and low feeds (Figure 2), while the 50% phenolic samples show minimum surface roughness values at low speeds and high feeds (Figure 3).

The Roughness Model: Using the experimental results, empirical equations have been obtained to estimate surface roughness as functions of the independent variables (i.e. speed and feed). The resulting models obtained using RSM are as follows:

<u>100% phenolic Sample:</u> The first order RSM model is given by:

$$Y_1 = Y - \in = 0.410923\, x_0 \;- 0.0027\, x_1 + 0.002791\, x_2 \tag{9}$$

The transformed equation of surface roughness prediction is as follows:

$$R_a = 1.207493\, v^{-0.017515}\, f^{0.01245} \tag{10}$$

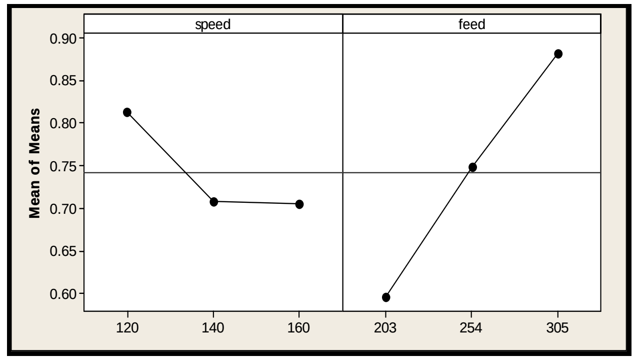

Figure 1. R_a Response Plot for 100% Phenolic Sample

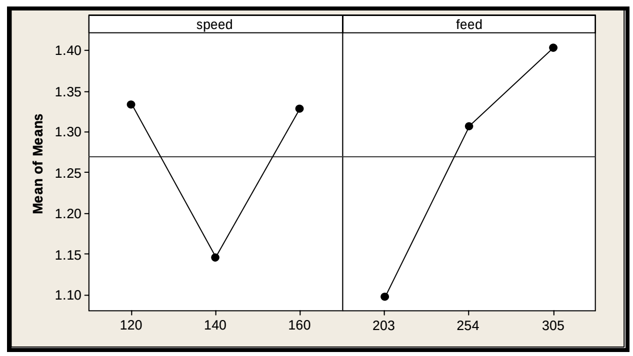

Figure 2. R_a Response Plot for 75% Phenolic Sample

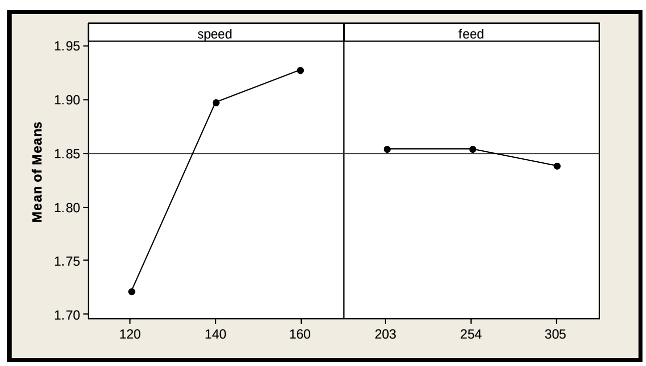

Figure 3. R_a Response Plot for 50% Phenolic Sample

Equation 10 is derived from 6 and 7 by substituting the coded values of x_1 and x_2 in terms of ln v and ln f. Results of ANOVA are shown in Table 3 below. Since the calculated values of the F-ratio are less than the standard values of the F-ratio for surface roughness (i.e., the P-value is less than 0.05), the model is adequate at the 95% confidence level to represent the relationship between the machining response and the machining parameters of the milling process. The multiple regression coefficient for the first order model was found to be 0.8862. This shows that the first order model can explain the variation in surface roughness to an extent of 88.62%.

Table 3. ANOVA Results for First Order Model - 100% Phenolic

	df	SS	MS	F	Prob>F	R^2
Regr	2	0.1391	0.0695	23.353	0.0015	0.8862
Resid	6	0.0179	0.0030			
Total	8	0.1569				

Since the first order model was not entirely sufficient, a second order model was then examined:

$$Y_2 = Y - \in = 0.965073\,x_0 - 0.02622\,x_1 + 0.01118\,x_2 + 0.000126\,x_1^2 + 0.0000038\,x_2^2 + 0.000046\,x_1 x_2 \quad (11)$$

The results for the ANOVA and F-test are shown in Table 4 below. Since the P-value was less than 0.05, there was a definite relationship between the response variable and independent variables at the 95% confidence level. The multiple regression coefficient of the second order model was found to be 97.60%. On the basis of the multiple regression coefficient (R^2), the second order model was considerably more adequate to represent this relationship.

Table 4. ANOVA Results for Second Order Model - 100% Phenolic

	df	SS	MS	F	Prob>F	R^2
Regr	5	0.1532	0.0306	24.3812	0.0123	0.9760
Resid	3	0.0038	0.0013			
Total	8	0.1570				

75% phenolic sample: The first order model obtained from the functional relationship (Equation 4) was:

$$Y_1 = Y - \in = 0.526967\,x_0 - 0.00011\,x_1 + 0.002983\,x_2 \quad (12)$$

The transformed equation of surface roughness prediction was thus:

$$R_a = 0.45677\,v^{-0.00071}\,f^{\,0.013309} \quad (13)$$

ANOVA and the F-ratio results are shown in Table 5 below. The P-value was greater than 0.05, so the model was not adequate at the 95% confidence level. The multiple regression coefficient for the first order model was found to be 36.24%. As it is not sufficiently adequate, the second order model was then examined.

Table 5. ANOVA Results for First Order Model - 75% Phenolic

	df	SS	MS	F	Prob>F	R^2
Regr	2	0.1389	0.0695	1.7053	0.2592	0.3624
Resid	6	0.2444	0.0407			
Total	8	0.3833				

The second order surface roughness model was:

$$Y_2 = Y - \in = 7.921301\,x_0 - 0.12814\,x_1 + 0.014657\,x_2 + 0.000462\,x_1^2 - 0.000022\,x_2^2 - 0.0000051\,x_1 x_2 \quad (14)$$

The results for the ANOVA and F-test for the second order model is shown in Table 6 below. The P-value was greater than 0.05, so the model was not adequate at the 95% confidence level. The second order model was slightly better than the first order, though, and had an R^2 of 55.73%.

Table 6. ANOVA Results for Second Order Model - 75% Phenolic

	df	SS	MS	F	Prob>F	R^2
Regr	5	0.2136	0.0427	0.7552	0.6353	0.5573
Resid	3	0.1697	0.0566			
Total	8	0.3833				

50% phenolic sample: The first order model is given by:

$$Y_1 = Y - \in = 1.168429x_0 + 0.005147x_1 - 0.00016x_2 \quad (15)$$

The transformed equation of surface roughness prediction is as follows:

$$R_a = 1.0073835\,v^{0.0333894}\,f^{-0.000713} \quad (16)$$

The ANOVA and F-ratio test results are shown in Table 7 below. Again it has been found that the P-value was greater than 0.05, so the model was not adequate at the 95% confidence level. The multiple regression coefficient for the first order model was found to be 47.87%, thus a second order model was considered.

Table 7. ANOVA Results for First Order Model - 50% Phenolic

	df	SS	MS	F	Prob>F	R^2
Regr	2	0.0640	0.0320	2.7549	0.1417	0.4787
Resid	6	0.0697	0.0116			
Total	8	0.1336				

The second order model was found to be:

$$Y_2 = Y - \in = -1.52417\,x_0 + 0.048853\,x_1 - 0.00262\,x_2 - 0.00018\,x_1^2 - 0.0000032\,x_2^2 + 0.000293\,x_1 x_2 \quad (17)$$

The data for ANOVA and F-test for the second order surface roughness is shown in Table 8 below. The P-value was greater than 0.05, so the model was not adequate at the 95% confidence level. The second order model was slightly better than the first order, and had an R^2 of 58.63%.

Table 8. ANOVA Results for Second Order Model - 50% Phenolic

	df	SS	MS	F	Prob>F	R^2
Regr	5	0.0784	0.0157	0.8503	0.5935	0.5863
Resid	3	0.0553	0.0184			
Total	8	0.1336				

Taguchi Analysis Results: The results for 100%, 75% and 50% phenolic are shown below in Tables 9 to 11, respectively. Based on these, contour plots of the surface roughness against speed and feed have been obtained and are shown in Figures 4 to 6. The response tables below show the average of each response characteristic for each level of each factor. The tables also include ranks based on the delta statistics, which compare the relative magnitude of the effects. The delta statistic is the highest minus the lowest average of each factor. In MINITAB, ranks are assigned based on delta values: rank 1 to the highest delta value, rank 2 to the second highest, and so on. The rank indicates the relative importance of each factor to another factor.

Table 9. Response Table for R_a Means - 100% Phenolic Sample

Level	Speed (m/min)	Feed (mm/min)
1	0.8128	0.5964
2	0.7085	0.7486
3	0.7048	0.8811
Delta	0.1080	0.2847
Rank	2	1

Table 10. Response Table for R_a Means - 75% Phenolic Sample

Level	Speed (m/min)	Feed (mm/min)
1	1.334	1.099
2	1.147	1.307
3	1.330	1.403
Delta	0.187	0.304
Rank	2	1

Table 11. Response Table for R_a Means - 50% Phenolic Sample

Level	Speed (m/min)	Feed (mm/min)
1	1.722	1.854
2	1.898	1.855
3	1.928	1.838
Delta	0.206	0.016
Rank	1	2

Summary

From these results, the combinations of speed and feed which caused the surface roughness values to decrease can be observed. The combinations of optimum speed and feed that increased the surface finish for the samples in this study are given below:

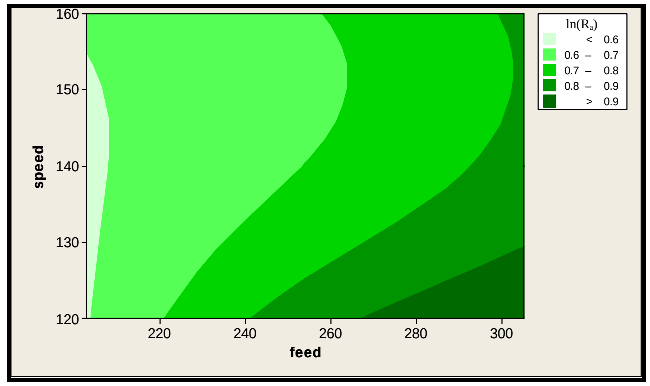

Figure 4. Contour Plot of $\ln(R_a)$ vs. Speed and Feed - 100% Phenolic Sample

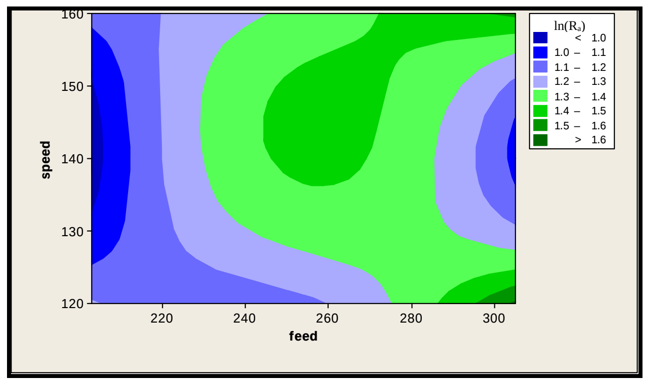

Figure 5. Contour Plot of $\ln(R_a)$ vs. Speed and Feed - 75% Phenolic Sample

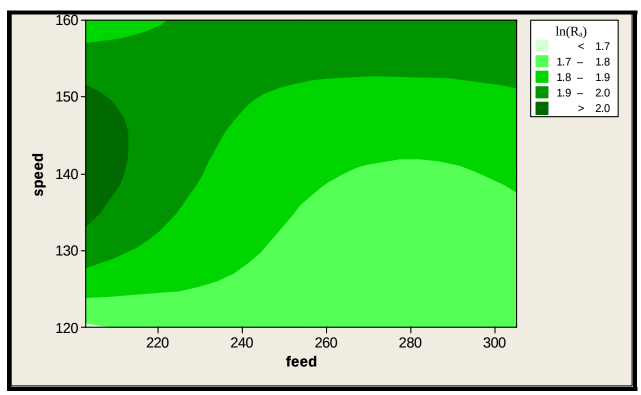

Figure 6. Contour Plot of $\ln(R_a)$ vs. Speed and Feed - 50% Phenolic Sample

- Contour surface plots of 100% phenolic samples show low surface roughness values at high speeds and low feeds. Therefore a better surface finish can be obtained at high speeds and low feeds. The Taguchi analysis shows that feed has relatively more impact on surface roughness compared to speed. The ANOVA results show that the first order fit is 88.6% accurate, while the second order is 97.6%. Thus the second order model explains a much higher proportion of the variability in the response.

- Contour surface plots of 75% phenolic samples do not follow any particular trend, but in general lower surface roughness values are obtained at high speeds and low feeds. The Taguchi analysis results show that feed has relatively more impact on surface roughness compared to speed. The ANOVA results show that the first order fit is 36.2% accurate, while the second is 55.7%, both of which are fairly low.
- Contour surface plots of 50% phenolic samples show low surface roughness values at low speeds and high feeds. The Taguchi analysis results show that speed has relatively more impact on surface roughness compared to feed. ANOVA results show that the first order fit is 47.9% accurate, while the second order is 58.6%, both of which are fairly low.

Although a concerted effort has been made to study the machinability of plastic composites filled with corn ethanol processing coproducts, further research is needed to refine the relationships between surface roughness and cutting speed and feed rate. Additional experiments will be carried out to improve the sensitivity of the results. Additionally, other variables to be considered for future studies include cutting force measurement and the determination of overall machinability indexes.

References

[1] Tatara, R. A., Suraparaju, S. and Rosentrater, K. A., "Compression molding of phenolic resin and corn-based DDGS blends", Journal of Polymers and the Environment, v 15, n 2, 2007, p 89-95.

[2] El baradie, M. A., "Surface Roughness model for turning grey cast iron (154 HN)" Proc. IMechE, v. 207, 1993, p 43-50.

[3] Mansour, A. and Abdalla, H., "Surface Roughness model for end milling: A semi-free cutting carbon casehardening steel (EN32) in dry condition", Journal of Materials Processing Technology, v 124, n 1-2, 2002, p 183-191

[4] Amago, T., "Sizing optimization using response surface method in First Order analysis". R & D Review of Toyota CRDL, v 37 n 1.

[5] Alauddin, M., El Baradie, M. A. and Hashmi, M. S. J., "Optimization of surface finish in end milling Inconel 718", Journal of Materials Processing Technology, v 56, n 1-4, 1996, p 54-65

[6] Keller, P., "Six Sigma demystified", McGraw-Hill, New York 2005, p 205-210.

[7] Reddy, N. S. K. and Rao, P. V., "Selection of optimum tool geometry and cutting conditions using a surface roughness prediction model for end milling", International Journal of Advanced Manufacturing Technology, v 26, 2005, p 1202-1210.

[8] Ross, P., "Taguchi techniques for quality engineering: loss function, orthogonal experiments, parameter and tolerance design", McGraw-Hill, New York, 1988.

[9] Datta, B. N. "Numerical Linear Algebra", 2005 p 265-301.

Acknowledgements

The authors are grateful to both the USDA – ARS as well as the NIU Department of Technology for funding, facilities, and equipment, all of which were essential in completing this research.

Mention of a trade name, proprietary product, or specific equipment does not constitute a guarantee or warranty by the United States Department of Agriculture and does not imply approval of a product to the exclusion of others that may be suitable.

Biographies

KURT A. ROSENTRATER, Ph.D., is a Lead Scientist with the United States Department of Agriculture – Agriculture Research Service, where he is developing value-added uses for residue streams from biofuel manufacturing operations. He is a former Assistant Professor in the Department of Technology at NIU. Dr. Rosentrater may be reached at kurt.rosentrater@ars.usda.gov

ANDREW OTIENO, Ph.D., is an Associate Professor in the Department of Technology at Northern Illinois University. He has done extensive research in analysis of machining problems and environmentally friendly manufacturing. His research and teaching interests include machine vision, materials and manufacturing processes, finite element analysis, and manufacturing automation. Dr. Otieno may be reached at otieno@ceet.niu.edu

PRATYUSHA MELAMPATI is a graduate student in the Department of Mechanical Engineering at NIU. She is currently working on the development of bio-based plastic materials as part of her MS thesis.

A Simple Deadlock Avoidance Algorithm in Flexible Manufacturing Systems

Paul E. Deering, Ohio University

Abstract

As flexible manufacturing systems (FMS) become more flexible and complex, the subject of deadlock avoidance becomes essential. This paper presents a simple yet effective algorithm that can be implemented at two levels of complexity to avoid deadlock in an FMS. This paper discusses the differences between primary deadlock and impending deadlock; it models an FMS using digraphs to calculate slack, knot, order, and space to avoid deadlock. Several examples are provided demonstrating the method.

Introduction

Allowing a manufacturing system to enter only live states (deadlock-free states) and avoid any dead states (deadlocked states) can save loss of production and labor costs, as well as provide better resource utilization. Moving the wrong part in a live FMS can cause deadlock that can both cripple the entire manufacturing system and stall production. The only recourse is to manually resolve the deadlock and reset the FMS to a known state that is live. To prevent manual deadlock resolution in an FMS, a deadlock avoidance algorithm that can determine which parts to move must be incorporated into the controller of the FMS.

There are two types of deadlock that can occur in a manufacturing system. The most basic type is primary deadlock. This situation occurs when each part on a circuit requests the next resource in its process plan. This situation is illustrated in Figure 1.

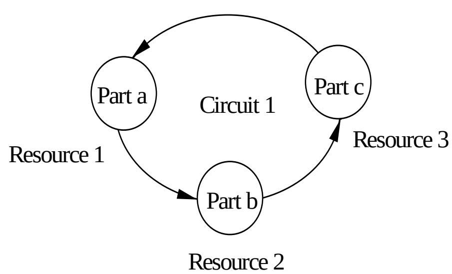

Figure 11. Example of Primary Deadlock

Assume that part a in resource 1 has to go to resource 2, part b in resource 2 has to go to resource 3, and part c in resource 3 has to go to resource 1 before each part is completed. If resource 1, resource 2, and resource 3 can only hold one part at a time, no parts can move without intervention. Circuit 1 in Figure 1 is said to be in primary deadlock.
A more complex and difficult-to-detect type of deadlock is called impending deadlock; this occurs when parts can move through the system but will terminate in primary deadlock after a finite number of moves. Consider the system shown in Figure 2 and assume that each resource can only hold one part. Assume that part *a* is occupying resource 1 and that part *a* first requires resource 2, then resource 3. Likewise, assume part *b* is occupying resource 3, and the next resource required by part *b* is resource 2 followed by resource 3. Although part *a* can move to resource 2, the system will terminate in primary deadlock on circuit 2. Part *b* can also move to resource 2, but primary deadlock will result on circuit 1.

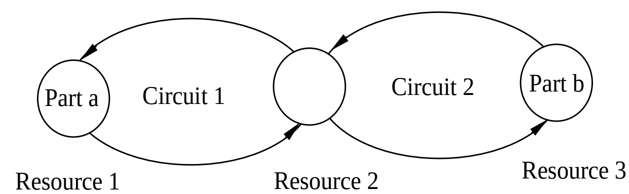

Figure 2. Example of Impending Deadlock

The two main approaches to solving the deadlock situation in manufacturing systems include: detection and resolution and avoidance. Deadlock detection and resolution methods [3, 4, 10, 13, 14] allow deadlocks to occur. The deadlock is resolved by implementing a deadlock recovery procedure that moves parts to buffers and resets the system to a live state. Deadlock avoidance methods [1, 2, 5, 6, 7, 8, 9, 11, 12, 15, 16, 17, 18] avoid deadlock by controlling the mix of parts in the system at any given time. A part can be moved or introduced into the system only if the move does not cause deadlock. If a move is found to cause deadlock, then the move is not allowed to occur, thus avoiding the deadlock state.

This paper presents the results of reference [16] and demonstrates a simple algorithm that can be implemented at two levels of complexity to avoid primary and impending deadlock. This paper is organized as follows: the first section discusses previous research on deadlock in a FMS; the next section defines a mathematical model of a manufacturing systems; circuit parameters slack, knot, order and space is then defined; the next section proves sufficient conditions for a deadlock-free system; several examples demonstrating the method is then provided; next the deadlock avoidance algorithm is presented; and finally concluding remarks about the method and future research.

Related Research

Many researchers use Petri nets [1, 2, 5, 10, 11, 12, 14] as a formalism to describe deadlock in a manufacturing system. Banaszak and Krogh [1] proposed a deadlock avoidance algorithm (DAA), which developed a restriction policy based on production route information to guarantee that no circular wait situations would occur. Their DAA is sufficient for avoiding deadlocks but is not an optimal solution. Viswanadham, Narahari, and Johnson [10] developed a deadlock avoidance algorithm that employed a look-ahead policy. This algorithm did not detect all deadlocked states, and the authors suggested using a recovery mechanism in case of system deadlock. Zhou and DiCesare [11] and Zhou [12] generalized the sequential mutual exclusions (SME) and parallel mutual exclusions (PME) concepts and derived the sufficient conditions for a Petri net (PN) containing such structures to be bounded, live, and reversible. In general, PN solutions are suitable for manufacturing systems that contain few resources but become very complicated for larger systems.

Another formalism to describe the manufacturing system is to use graphs [3, 4, 6, 7, 8, 9, 13, 14, 15, 16, 17, 18, 19]. In this approach, the vertices represent resources and the edges represent part flows between resources. Wysk, Joshi, and Yang [13] were the first to develop a specialized directed graphical structure called a wait relation graph (WRG) to model a manufacturing system. In reference [13], they developed a string manipulation procedure that yields a set of control actions to detect and recover from primary deadlock. Cho, Kumaran, and Wysk [3] used system status graphs to develop the concept of simple and non-simple bounded circuits with empty and non-empty shared resources to detect part flow deadlock and impending part flow deadlock. This method introduced the concept of a bounded circuit to detect deadlock. The method detected deadlock based on characteristics of this bounded circuit. The methods in references [13] and [3] could only handle single capacity resources. Fanti, Maione, and Turchiano [4] used a graph called working procedure digraph and developed a simple graph-theoretic method for deadlock detection and recovery in systems with multiple capacity resources. This algorithm did not prevent deadlock from occurring either, but it suggested a suitable recovery strategy.

Judd and Faiz [6] expanded on the original formulation proposed by reference [13] and the first to define slack, order, and space to avoid deadlock. This method provided sufficient conditions for deadlock by satisfying a set of linear inequalities. Lipset, Deering, and Judd [8] extended reference [6] to precisely quantify necessary and sufficient conditions for deadlock to exist. In this research, they redefined the order of a knot, defined a special state called an evaluation state, and defined the concept of order reduction. The approach was to put the system into an evaluation state and then compute the order. Deering [16] improved reference [8] by further refining the order of a knot and evaluation state, as well as eliminating the need for order reduction. Zhang, Judd, and Deering [15] developed a deadlock avoidance algorithm (DAA) based on references [8] and [16], which avoided deadlock and was executed in polynomial time. Zhang, Judd, and Deering [18] expanded upon references [15] and [16] to quantify the sufficient conditions for a system state to be live and derived the liveness necessary and sufficient conditions for an evaluation state. Zhang and Judd [19] extended reference [18] to allow choice in process flow or flexible part routing.

Modeling a Manufacturing System

An FMS consists of a set, *R*, of finite resources, such as robots, buffers, and machines, which produce a finite set, *P*, of products. Each resource $r \in R$ has a capacity of cap(*r*) units that can perform the required operations. The capacity function can be extended to a set of resources, that is:

$$\text{cap}(R_1) = \sum_{\forall r \in R_1} \text{cap}(r), \quad \text{for any } R_1 \subseteq R. \tag{1}$$

For each product $p \in P$, the process plan $\text{plan}(p) = r_1 r_2 \ldots r_m$ defines the sequence of resources that are required to produce *p*. Resource r_m is the terminal resource for product *p*. It is assumed that all process plans are fixed, finite, and sequential. A part is an instance of a product that flows through the system. At any given time, a manufacturing system is working on a set Q of parts. The function $\text{class}(q)$ returns the product *p* to which part *q* belongs.

A manufacturing system can be represented by a WRG, $G = (V, A)$. Each vertex represents a resource; that is, *V*=*R*. A directed arc is drawn from vertex r_1 to vertex r_2, if r_2 immediately follows r_1 in at least one process plan. Each arc will be labeled with the part(s) that will flow through it. A subgraph $G_1 = (R_1, A_1) \subset G$ of an WRG consists of a subset of the resources and arcs of *G*, so that all the arcs in A_1 connect resources in R_1. The union (intersection), denoted by $G_1 \cup G_2$ $(G_1 \cap G_2)$, of two subgraphs is the union (intersection) of the component resource and arc sets. A path

$P=(R_p,A_p)$ is a subgraph whose resources and arcs can be ordered in the list $r_1a_1r_2a_2\ldots a_{n-1}r_n$ where each arc in the list connects the resources on either side. When specifying a path, writing the arcs is redundant. Therefore, only the resources will be enumerated when a path is defined. A simple path is a path with no repeated elements in the ordered list. A closed path is a path with the same first and last element. A simple circuit is a closed path with no repeated elements in the ordered list, except the first and last elements.

The function $\mathrm{n}(q)$ returns a positive integer that represents the position in $\mathrm{plan}[\mathrm{class}(q)]$ of the operation that is currently processing *q*. When a new part q is added to the system, then $\mathrm{n}(q)=1$. As the part is moved from resource to resource according to its plan, $\mathrm{n}(q)$ is incremented until it reaches the end of its plan and exits the system. The state *n* of a manufacturing system is a vector containing the current n(*q*) for all $q\in Q$. A state *n* of a manufacturing system is live if a sequence of part movements exist that will empty the system. A state *n* of a manufacturing system is dead, or deadlocked, if it is not live.

Given a manufacturing system $G=(R,A)$, let $a\in A$ and $r\in R$. Then, the function $\mathrm{tail}(a)$ returns the resource at the tail of the given arc; the function $\mathrm{head}(a)$ returns the resource at the head of the arc. A unit of the resource $r=\mathrm{tail}(a)$ is said to be committed to arc *a* if it is processing a part *q* whose next resource in its process plan is $\mathrm{head}(a)$. It is important to note that the number of resource units committed to the outgoing arcs of *r* can be less than the number of busy units. This happens when some of the busy units are being used for terminal operations. A resource unit is free if it is not committed to an arc; by this definition, a busy unit that is not committed is still termed free. A resource is free if any of its units are free. A resource is empty if it contains no parts. The commitment function $\mathrm{com}(a,n)$ returns the number of resource units that are committed to arc *a* when the system is in state *n*. The commitment function is extended to a set of arcs as follows:

$$\mathrm{com}(A_1,n)=\sum_{\forall a\in A_1}\mathrm{com}(a,n),\quad \text{for any } A_1\subseteq A \qquad (2)$$

A part is enabled if either the next resource in its process plan contains at least one resource unit that is not busy, or the part is in the last step of its process plan. Suppose that the system is in state n_0; there exists an arc *a* such that resource $r_2=\mathrm{head}(a)$ is free and the part in the resource $r_1=\mathrm{tail}(a)$ is committed to *a*. Then, when r_1 finishes its operation, this part can be moved to resource r_2. This process is called propagation. The symbol n_k is used to denote the state of the system after the k^{th} propagation. A part *q* in WRG G can be shifted to resource *r* if it can be propagated to *r* without propagating any other part in *G*. A part *q* in WRG G is said to have a free exit if it can shift its terminal resource r_m in *G*.

Slack, Knot, Order, and Space

This section will summarize the major concepts and results from [6, 8, 13, 16]. This section defines the concept of slack, knot, order, and space.

The slack is the number of free resource units available for parts to flow on a subgraph.

Definition 1: The slack of any subgraph $G_1=(R_1,A_1)\subseteq G$ is given by:

$$\mathrm{slack}(G_1,n)=\mathrm{cap}(R_1)-\mathrm{com}(A_1,n) \qquad (3)$$

A closed path *c* in a WRG *G* is in primary deadlock in state *n* if $\mathrm{slack}(c,n)=0$.

An interesting phenomenon happens when two simple circuits are joined by a single capacity resource as opposed to a multiple capacity resource. Consider the two manufacturing systems depicted in Figure 3 and Figure 4. Here, two simple circuits are joined by resource r_0, and all parts are committed to their outgoing arcs. In Figure 3 and Figure 4, the labels indicating which parts flow through each arc have been left off for simplicity.

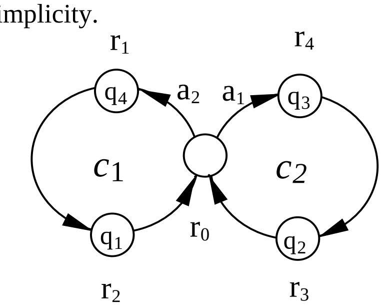

Figure 3. Two Simple Circuits Intersecting at a Single Capacity Resource

Assume that all resources in both systems are of a capacity of one, except where $\mathrm{cap}(r_0)=2$ and part q_5 is committed to arc a_1 (see Figure 4.) Further, assume in both systems that if q_1 is moved to resource r_0, it will be committed to arc a_1, and if part q_2 is moved to resource r_0, it will be committed to arc a_2.

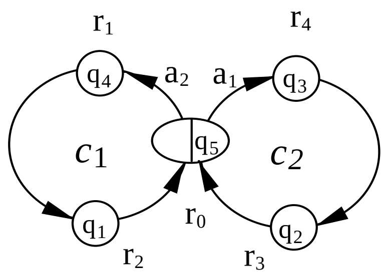

Figure 4. Two Simple Circuits Intersecting at a Multiple Capacity Resource

Even though resource r_0 is free in both manufacturing systems, Figure 3 shows a dead system, and Figure 4 shows a live one. In Figure 3, if either part q_1 or q_2 is moved into r_0, then primary deadlock will result on circuit c_2 or c_1, respectively. In Figure 4, if part q_1 were moved into r_0, then primary deadlock will result on circuit c_2. However, moving part q_2 will not cause deadlock, since this move will allow the parts to propagate along circuit c_2. This observation motivates the following definitions.

Definition 2: Let c_1 and c_2 be any two closed paths in a WRG of a manufacturing system. If $c_1 \cap c_2$ consists of exactly one resource with a capacity of one, then this resource is called a *knot* with respect to $c_1 \cup c_2$.

Clearly, r_0 in Figure 3 is a knot with respect to $c_1 \cup c_2$, since cap(r_0) = 1 and $c_1 \cap c_2 = r_0$. Resource r_0 in Figure 4 is not a knot, since cap(r_0) = 2. The next two definitions are needed to define the order of a knot.

Definition 3: Let c_1 and c_2 be two closed paths in a WRG *G*. Path c_1 is connected to c_2 if $c_1 \cap c_2 \neq 0$ and a part currently exists in the system that must propagate from c_1 to c_2 without leaving $c_1 \cup c_2$.

Definition 4: Given two closed paths c_1 and c_2, then c_1 and c_2 are cross-connected if c_1 is connected to c_2 and c_2 is connected to c_1.

Definition 5: Let the closed path *c* in state *n* consist of two closed paths, c_1 and c_2, such that $c = c_1 \cup c_2$ and $c_1 \cap c_2 = k$, where *k* is a knot. The order of knot *k* with respect to the closed path c in state *n* is defined as:

$$\text{order}(k,c,n) = \begin{cases} 1, \text{if } c_1 \text{ and } c_2 \text{ are cross connected.} \\ 0, \text{otherwise.} \end{cases} \quad (4)$$

The order of any simple circuit is zero.

The order of r_0 in Figure 3 is one, since c_1 and c_2 are cross-connected, that is $\text{order}(r_0, c_1 \cup c_2, n) = 1$.

Definition 6: Let *c* be a closed path in a WRG *G* in state *n* that contains *m* knots. Then, the order of *c* is given by: style:

$$\text{order}(c,n) = \sum_{i=1}^{m} \text{order}(k_i, c, n) \quad (5)$$

Definition 7: Let *c* be a closed path in a WRG *G* of a manufacturing system in state *n*. The free space on a closed path *c* is the difference between the slack and the order: style:

$$\text{space}(c,n) = \text{slack}(c,n) - \text{order}(c,n) \ \ \forall c \in C_G \quad (6)$$

where C_G is the set of all closed paths in *G*.

The following theorem proves that if all closed paths of a WRG *G* have space greater than zero, *G* is live.

Theorem 1: Let C_G be the set of all closed paths in a non-empty WRG *G* in state *n*. If,

$$\text{space}(c,n) > 0 \quad \forall c \in C_G \quad (7)$$

then *G* is live.
Proof: See reference [16].

Examples

This section consists of three examples demonstrating the method. The third example will show a condition where a live system has been evaluated to be dead.

Example 1: Let the WRG *G* in Figure 5 be in state *n*. The manufacturing system is composed of six resources, r_1, r_2, r_3, r_4, r_5, and r_6, all with unit capacity. The system contains seven closed paths. Let C_G represent the set of closed paths in *G*, such as $C_G = \{c_1, c_2, c_3, c_1 \cup c_2, c_1 \cup c_3, c_2 \cup c_3, c_1 \cup c_2 \cup c_3\}$
Suppose that the system manufactures three products, p_1, p_2 and p_3, specified by the following process plans: $\text{plan}(p_1) = r_1 r_6 r_2 r_3$, $\text{plan}(p_2) = r_3 r_4 r_6 r_5$, and $\text{plan}(p_3) = r_5 r_6 r_1$. Assume that parts *a*, *b*, and *c* belong to product classes p_1, p_2 and p_3, respectively. Suppose that the system is in state $n = [\text{n}(a), \text{n}(b_1), \text{n}(b_2), \text{n}(c)] = [1,2,1,1]$.

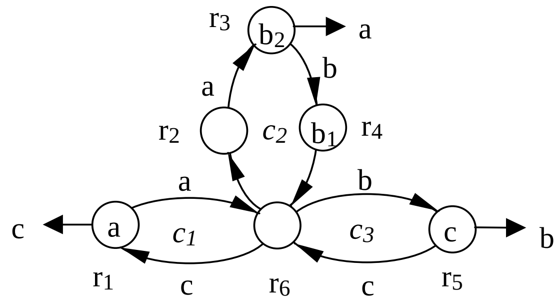

Figure 5. Manufacturing System for Example 1

Table 1 shows the capacity, commitment, slack, order, and space computations in state n.

Table 1. Circuit Parameters for Example 1

Subgraph	Capacity	Commitment	Slack	Order	Space
c_1	2	1	1	0	1
c_2	4	2	2	0	2
c_3	2	1	1	0	1
$c_1 \cup c_2$	5	3	2	0	2
$c_1 \cup c_3$	3	2	1	0	1
$c_2 \cup c_3$	5	3	2	0	2
$c_1 \cup c_2 \cup c_3$	6	4	2	1	1

Clearly, the space of all closed paths is greater than zero. The manufacturing system is live according to Theorem 1. Table 2 shows one possible sequence of moves to empty the system.

Table 2. Part Movements to Empty System in Example 1

Part Movement	Resulting State After Move
a to r_6	2 2 1 1
a to r_2	3 2 1 1
c free exit	3 2 1 -
b_1 free exit	3 - 1 -
b_2 free exit	3 - - -
a free exit	- - - -

Example 2: Let the WRG G in Figure 6 be in state n_0. The process plans for parts *a*, *b*, and *c* are presented in Table 3. Let $c_1 = r_1r_4r_2r_1$, $c_2 = r_2r_3r_4r_2$, and $c_3 = r_4r_5r_6r_4$. Assume that the state of the system is $n_0 = [n(a_1), n(a_2), n(b), n(c)] = [2, 1, 2, 1]$.

Table 3. Process Plans for Example 2

Part	Process Plan
a	$r_2r_1r_4r_2$
b	$r_2r_3r_4r_5r_6$
c	$r_6r_4r_2$

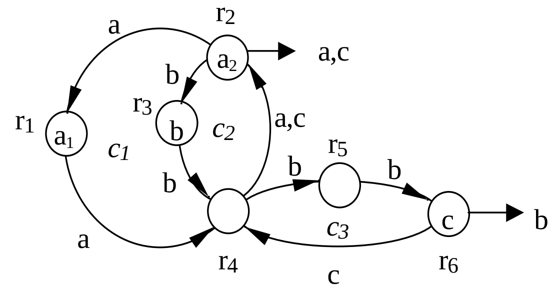

Figure 6. Manufacturing System for Example 2

Table 4. Circuit Parameters for Example 2

Subgraph	Capacity	Commitment	Slack	Order	Space
c_1	3	2	1	0	1
c_2	3	1	2	0	2
c_3	3	1	2	0	2
$c_1 \cup c_2$	4	3	1	0	1
$c_1 \cup c_3$	5	3	2	0	2
$c_2 \cup c_3$	5	2	3	1	2
$c_1 \cup c_2 \cup c_3$	6	4	2	1	1

Clearly, the space of all closed paths is greater than zero. The manufacturing system is live according to Theorem 1. Table 5 shows one possible sequence to empty the system.

Table 5. Part Movements to Empty System in Example 2

Part Movement	Resulting State After Move
a_1 to r_4	3 1 2 1
a_2 to r_1	3 2 2 1
a_1 free exit	- 2 2 1
a_2 free exit	- - 2 1
b to r_4	- - 3 1
b to r_5	- - 4 1
c free exit	- - 4 -
b free exit	- - - -

Example 3: Theorem 1 can conclude that a system is live if the space of all closed paths is greater than zero. If the space is zero, the system may be live or dead. Consider the following two cases.

Case 1: Suppose that the system in Figure 7 has the process plans depicted in Table 6.

Table 6. Process Plans for Example 3

Part	Process Plan
a	$r_1r_2r_3r_4r_6$
b	$r_5r_3r_4r_2r_1$
c	$r_6r_4r_2r_3r_5$

Assume that the system is in state $n=[a,b,c]=[1,1,1]$.

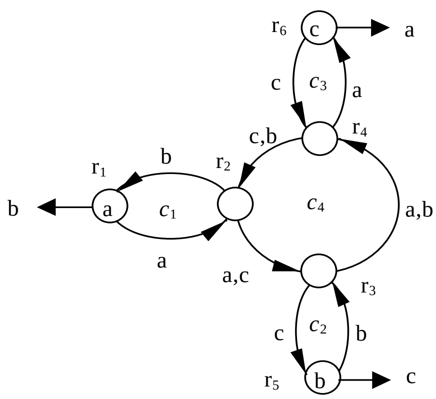

Figure 7. Manufacturing System for Example 3, Case 1

The space of all closed paths in Figure 7 is greater than zero, except for the closed path that contains the entire system, $\text{space}(c_1 \cup c_2 \cup c_3 \cup c_4, n_0) = 0$. Even though the space is zero, the system is live. Now, consider a WRG with the same structure, except for a different system state and part routings.

Case 2: Suppose the system in Figure 8 has the process plans as depicted in Table 7.

Table 7. Process Plans for Example 3

Part	Process Plan
a	$r_1r_2r_3r_5$
b	$r_5r_3r_4r_6$
c	$r_6r_4r_2r_1$

Assume that the system is in state
$n=[n(a),n(b),n(c)]=[1,1,1]$.

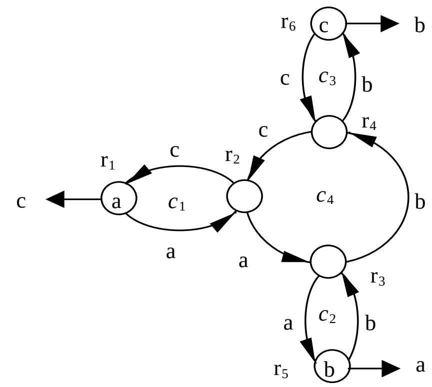

Figure 8. Manufacturing System for Example 3, Case 2

As in Case 1, the space of all closed paths in Figure 8 is greater than zero, except for the closed path that contains the entire system, $\text{space}(c_1 \cup c_2 \cup c_3 \cup c_4, n_0) = 0$. In this case, the system is dead. The space condition cannot distinguish between the two cases.

The Deadlock Avoidance Algorithm

An algorithm that implements the methods presented herein can be applied to any process control systems to avoid deadlock. The algorithm ensures that propagating an enabled part would not transition a live system to a dead state. The algorithm can be implemented in two different levels. A first level implementation, which is less restrictive, would be to define the order of all knots to one. A second level of implementation would compute the order of each knot per Definition 5. Implementing the algorithm at this second level would allow more live states but would add more complexity. A flowchart of these two implementations is depicted in Figure 9.

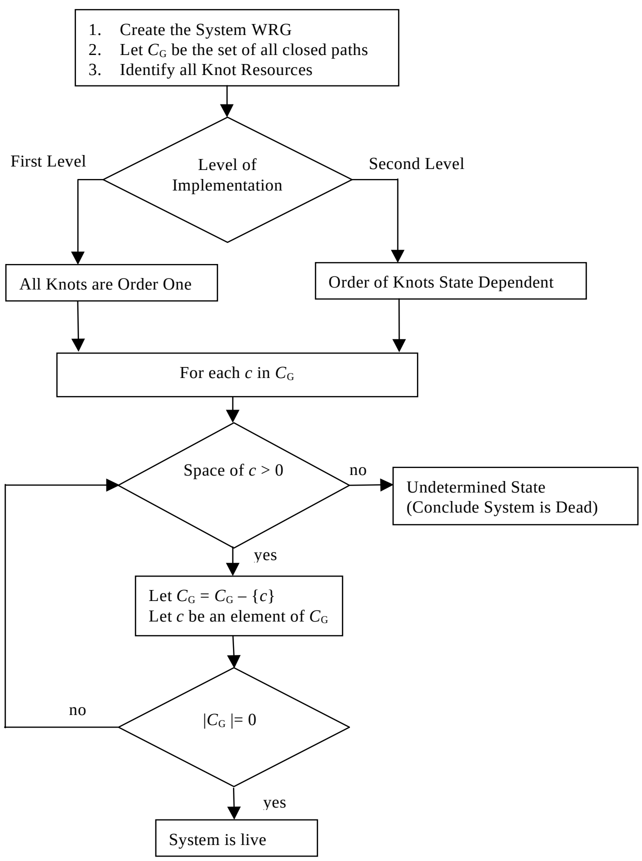

Figure 9. First and Second Level Implementation Flowchart

Conclusion

A deadlock avoidance algorithm was developed that avoids both primary and impending deadlock in an FMS. The concepts of slack, knot, order, and space were derived from circuit observations and interactions using WRGs. The algorithm ensures deadlock is avoided by not allowing a live system to enter dead states by satisfying a set of linear inequalities, *space* > 0 for all closed paths.

The algorithm detects all dead states. The algorithm does not detect all live states, as shown in Example 3. A special state called the evaluation state, presented in references [16] and [18], is necessary to determine the liveness of these indistinguishable states. This will be addressed in future publications.

Reference

[1] Banaszak, Z. and B. Krogh (1990), "Deadlock Avoidance in Flexible Manufacturing Systems with Concurrently Competing Process Flows." IEEE Trans. on Robotics and Auto., vol. 6, no. 6, pp. 724–733.

[2] Barkaoui, K. and I.B. Abdallah. (1995), "A Deadlock Method for a Class of FMS," Proceedings of the 1995 IEEE Int. Conf. On Systems, Man and Cybernetics, pp. 4119–4124.

[3] Cho, H., T.K. Kumaran, and R. Wysk (1995), "Graph-Theoretic Deadlock Detection and Resolution for Flexible Manufacturing Systems," IEEE Trans. on Robotics and Auto., vol. 11, no. 3, pp. 550–527.

[4] Fanti, M., G. Maione, and B. Turchiano (1996), "Deadlock Detection and Recovery in Flexible Production Systems with Multiple Capacity Resources," Industrial Applications in Power Systems Computer Science and Telecommunications Proceedings of the Mediterranean Electrotechnical Conference, vol. 1, pp. 237–241.

[5] Hsieh, F. and S. Chang (1994), "Dispatching-driven Deadlock Avoidance Controller Synthesis for Flexible Manufacturing Systems," IEEE Trans. Robotics and Auto., vol. 10, no. 2, pp. 196–209.

[6] Judd, R. P. and T. Faiz (1995), "Deadlock Detection and Avoidance for a Class of Manufacturing Systems," Proceedings of the 1995 American Control Conference, pp. 3637–3641.

[7] Judd, R. P., P. Deering, and R. Lipset (1997), "Deadlock Detection in Simulation of Manufacturing Systems," Proceedings of the 1997 Summer Computer Simulation Conference, pp. 317–322.

[8] Lipset, R., P. Deering, and R. P. Judd (1997), "Necessary and Sufficient Conditions for Deadlock in Manufacturing Systems," Proceedings of the 1997 American Control Conference, vol. 2, pp. 1022–1026.

[9] Lipset, R., P. Deering, and R. P. Judd (1998), "A Stack-Based Algorithm for Deadlock Avoidance in Flexible Manufacturing Systems," Proceedings of the 1998 American Control Conference.

[10] Viswanadham, N., Y. Narahari, and T. Johnson. (1990). "Deadlock Prevention and Deadlock Avoidance in Flexible Manufacturing Systems Using Petri Net Models," IEEE Trans. on Robotics and Auto., vol. 6, no. 6, pp. 713–723.

[11] Zhou, M. and F. DiCesare (1992), "Parallel and Sequential Mutual Exclusion for Petri Net Modeling of Manufacturing Systems with Shared Resources," IEEE Trans. on Robotics and Auto., vol. 7, no. 4, pp. 550–527.

[12] Zhou, M. (1996), "Generalizing Parallel and Sequential Mutual Exclusions for Petri Net Synthesis of Manufacturing Systems," IEEE Symposium on Emerging Technologies and Factory Automation, vol. 1, pp. 49–55.

[13] Wysk R., N. Yang, and S. Joshi (1991), "Detection of Deadlocks in Flexible Manufacturing Systems," IEEE

Transactions Robotics and Automation, vol. 7, no. 6, pp. 853–858.
[14] Ezpeleta, J., J. Colom, and J. Martinez (1995), "A Petri Net Based Deadlock Prevention Policy for Flexible Manufacturing Systems," IEEE Trans. on Robotics and Automation, vol. 11, no. 2, pp. 173–184.
[15] Wenle, Z., R. P. Judd, and P. Deering (2003), "Evaluating Order of Circuits for Deadlock Avoidance in a Flexible Manufacturing System," Proceedings of the 2003 American Control Conference, pp. 3679–3683.
[16] Deering, E. P. (2000), Necessary and Sufficient Conditions for Deadlock in Manufacturing Systems, PhD Dissertation, Ohio University.
[17] Fanti, M.P., B. Maione, S. Mascolo, and B. Turchiano (1995), "Control Polices Conciliating Deadlock Avoidance and Flexibility in FMS Resource Allocation," IEEE Symposium on Emerging Technologies and Factory Automation, vol. 1, pp. 343–351.
[18] Wenle, Z., R. P. Judd, and P. Deering (2004), "Necessary and Sufficient Conditions for Deadlocks In Flexible Manufacturing Systems Based On A Digraph Model," Asian Journal of Controls, vol. 6, no 2, pp. 217–228.
[19] Wenle, Z. and R. P. Judd (2007), "Evaluating Order Of Circuits For Deadlock Avoidance in a Flexible Manufacturing System," Asian Journal of Controls, vol. 9, no. 2, pp. 111–120.

Biographies

PAUL DEERING received his B.S. in Electrical Engineering, M.S. in Mathematics and Computer Science and Ph.D. in Engineering from Ohio University. He is currently an Assistant Professor in the Industrial Technology Department in the Russ College of Engineering and Technology at Ohio University. He has worked in the area of Information Technology for more than 20 years and has taught many engineering and computer science courses. Dr. Deering may be reached at deering@ohio.edu

IMPLEMENTING AN ADAPTIVE ROBOT WITH MULTIPLE COMPETING OBJECTIVES IN A SERVICE INDUSTRY ENVIRONMENT

Fletcher Lu, University of Ontario Institute of Technology; Lorena Harper, University of Maryland Eastern Shore

Abstract

This research paper presents the implementation of an adaptive learning algorithm from artificial intelligence known as Reinforcement Learning in a robot that must deal with more than one reward where the rewards may come into conflict with each other. A case that practically illustrates this problem is in a service industry environment where a robot is implemented to pick up objects for cleaning and/or attending to clients. An example of conflicting rewards for this application would be achieving a high reward for quickly picking up objects which typically conflicts with minimizing any damage inflicted on the object during the picking up process.

The innovative component of our research is that we will use multiple competing rewards for some states in contrast to the single reward per state method traditionally used in Reinforcement Learning. We compare these two approaches through the implementation of a Lego Mindstorm robot that has been programmed with both learning methods. The objective of our robot is to pick up objects quickly without damaging the object. We illustrate the conditions under which it is advantageous to use a single state for competing rewards over a multi-state approach through practical comparisons on efficiency for our Lego robot.

The objective of this research is to broaden the adaptability of learning robots. The impact on service industries, such as hotel and restaurant service, of this research would be to increase the acceptability of adaptable robots into fields of manual labor that have traditionally been limited due to the inflexibility of robots in dealing with dynamic situations.

Introduction

Although robots have been used to perform tasks since the beginning of the industrial age, it is only in the past 20 years, since the advent of artificial intelligence research, that robots can handle tasks that are not completely repetitive [1]. A learning robot fundamentally differs from a robot that performs a repetitive task in that the learning robot can modify its behavior with sensory feedback. One of the most popular learning methods for implementing such robots is the Reinforcement Learning system [1]. This approach has been used to implement robots that can act as tour guides [2], robotic nurses [3], and automobile drivers [4]. The learning component of these robots makes them more flexible so that they can modify their behavior.

Reinforcement Learning operates by modeling the environment as a network of states, S, where actions, A, can be taken to move from one state to another. Rewards, R, are associated with each state and the general goal is to maximize the long-term rewards one may obtain as one navigates through the environment. In order to achieve this goal one needs to develop a function known as a 'policy' (represented by the symbol π) which maps states to action: $\pi(S) \longrightarrow A$. The main objective is to find what is known as an optimal policy, π^* that produces the best long-term rewards navigating through the environment using function π^* [5].

The Reinforcement Learning approach to modeling the world and developing an optimal policy works very well for a broad range of applications. However it is generally limited in the sense that it assumes a single reward for any given state [6] [7]. There are a variety of situations where this is not necessarily the case. For instance, in a service industry robot, we may wish to implement a robot that can pick up objects for cleaning purposes, such as cleaning up hotel rooms. One natural single state is to have successfully grabbed an object for pick up. For an efficient cleaning robot to achieve this state of successfully grabbing an object for pick up, two problems however must be overcome. First, enough pressure must be applied to the object with the robot's grabbing apparatus so that the object does not slip through. Second, excessive amounts of pressure must not be applied or the robot would damage the object.

These two challenges can be viewed as competing rewards to achieve the same state. This state is the grabbing of the object, which is essentially applying just the right pressure to pick up the object without damaging it. The competing computed rewards would be, the more pressure applied, the greater the chance of successfully picking up the object, with an opposing reward of the less pressure applied, the greater the chance of successfully not damaging the object for pick up.

An alternative approach, which is often used, is to split the two competing rewards into separate states, one state for each reward. However this is not a natural solution for many real situations such as the cleaning robot problem. For the cleaning robot problem, for instance, the state of the amount of pressure applied to pick up an object is more naturally a single state.

The primary goal of this research is to discern the advantages of combining competing rewards in a single state versus separating the rewards into separate states. We also will determine the conditions under which it is more efficient to use separate states for each competing reward versus our combined reward/single state alternative.

The major benefit to adding in a multiple reward structure for each state is that we provide more options in implementing robots. This greater flexibility in implementation allows for greater adaptability in learning robots.

Background on Reinforcement Learning

A Reinforcement Learning system models the environment as a network of states, where transitions from one state to the next follow a Markov reward process on a finite set of N states. Recall that we transition from one state to another by choosing an action that moves us into another state, given the current state we are in and the action chosen. This produces a set of transition probabilities. We choose actions based on a policy function π, which maps states to actions. The goal is to find an optimal policy that produces the best long-term rewards [1]. To do so, we start by arbitrarily choosing a policy and evaluating it for long-term rewards. This evaluation is possible due to the Markov process assumption [8].

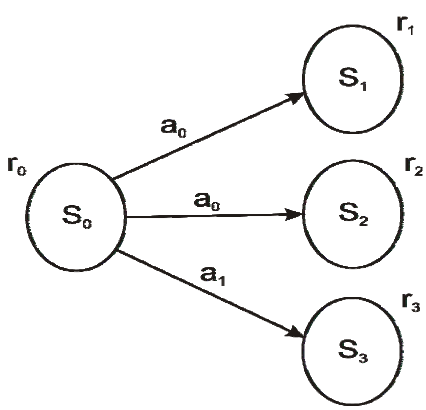

Figure 1. Program Flow Chart

A Markov process implies that in a given state, n, one transitions to a next state, m, by the conditional probability model $P(S_{i+1}=m|S_i=n)$, where we assume the transition probabilities do not change over process time i (stationarity assumption) [9]. Such a transition model can be represented by an N x N matrix P, where P(n,m) denotes $P(S_{i+1}=m|S_i=n)$ for all process times i. The reward R_i observed at time i is independent of all other rewards and states given the state S_i visited at time i. We also assume the reward model is stationary and therefore let r(n) denote $E[R_i|S_i=n]$ and s(n) denote $var(R_i|S_i=n)$ for all process times i. Thus, r and s represent the vectors (of size N x 1) of expected rewards and reward variances respectively over the different states n=1,...,N.

The value function v(n) is defined to be the expected sum of rewards obtained by starting in a start state S_0=n. That is, v is a vector given by:

$$v = r + \gamma \Pr + \gamma^2 \Pr + \ldots \qquad (1)$$

where $0<\gamma<1$ is a discounting term used on the rewards.

We can solve this equation by substituting the infinite sequence with vector v to produce the equation:

$$v = r + \gamma P v \, . \qquad (2)$$

Therefore, if P and r are known then v can be calculated explicitly by solving the matrix equation:

$$(I - \gamma P)v = r \, . \qquad (3)$$

We compute an estimate of the transition probabilities to produce our matrix P during our learning phase of the learning algorithm. With our estimate of P and the rewards we collect during the learning phase to produce the vector r, we can create an estimate of the long-term rewards through the value function v [5]. All these values are dependent on the fixed policy function π. Once we have evaluated this policy, we can then iteratively improve it by modifying the policy for each state to choose a better action giving improved long-term rewards. It has been proven that one can non-trivially improve a policy at every iteration of this process until an optimal policy has been reached [11].

A variety of approaches may be implemented to choose actions for states during the learning phase of the Reinforcement Learning algorithm. For our implementation we will use a random uniform probability method to choose among all possible actions.

When implementing a real-world robot using Reinforcement Learning, most approaches use the single reward per state method [2][12]. However, in a real-world environment, such restrictions are very limiting when attempting to simulate a more dynamic robot that can adapt to gradient conditions such as different degrees of pressure and temperature. The situation is especially challenging when attempting to deal with ultimately developing humanoid type robots such as those considered by Peters et al. [13].

Later robotic implementations dealing with more complex environments have created more complex functional type rewards without explicitly considering benefits and drawbacks of actually splitting the rewards into multiple states. Zhumatiy et. al. [14], for instance created a robot with a functional reward dependent on both an obstacle and target value. Our contribution is thus to consider such benefits and drawbacks to single function rewards versus splitting the reward into multiple states.

Lego Robots

For our robotic implementation, we used the Lego Mindstorm NXT kit to build our robot. The NXT kit includes several essential components in order for it to be useful as a learning robot. The most important components are the sensors that allow for feedback to our robot to sense the state of its environment. Without such sensors, it would be impossible to learn whether actions taken by the robot would be yielding positive or negative results. There are three sensors that were used in our robot implementation: (1) a light sensor that could send out a laser beam of light and measure the amount of reflected light when the beam hits an object, (2) an ultrasonic sensor that is used to measure distance by an approach similar to sonar detection, whereby distance is measured by measuring the time needed for an ultrasonic wave to be reflected back to the sensor, and (3) a touch sensor, which can measure the degree to which the sensor button is pressed. In addition to these sensors, the robot includes servomotors, which are essential in our robotic implementation, so that we can apply continuous pressure through the motors on an object without destroying the motors themselves.

In addition to the hardware of the NXT kit that made the robot learning possible, is the software component. The standard Graphical User Interface system for programming NXT robots is very limited. However, Lego allows for others to develop programming compilers for its system by making its byte code available for translation. In our case, we used the NXC programming language, which stands for Not eXactly C [15]. This language allows for the creation of arrays, which are essential for the matrix vector computations in the Reinforcement Learning algorithm. In addition, it includes random number generators and probability computations needed for our uniform random choices during our learning phase as well as the computations of the probability matrix P. Also the language allows for concurrent programming mechanisms such as semaphores and mutexes to avoid multiple simultaneous accesses to controlled systems such as motors.

Our Picking-Up Robot

For our robot implementation, we wished to create a robot that could pick up objects. The variables included:
1. the amount of pressure the robot could apply to the object in order to pick it up and 2.the speed at which it would try to pick up the object. The robot needed to be able to sense if the object was being damaged during its picking up process, as well as whether it had dropped the object because the pressure it was applying was insufficient to hold the object.

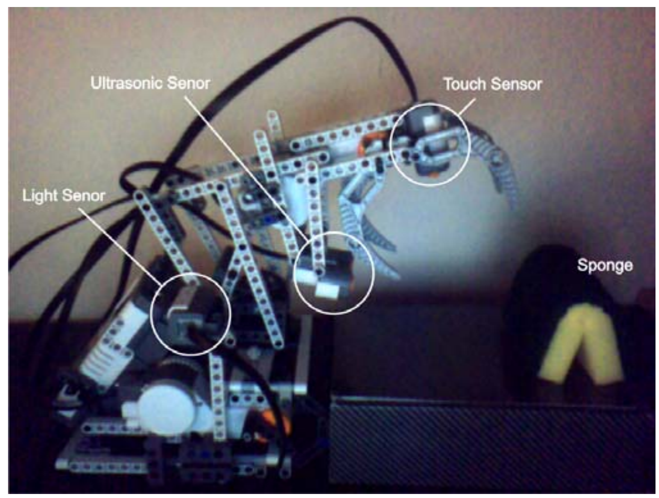

Figure 2. Picking-Up Robot

Figure 2 shows our completed robot. The arm of the robot has both the touch sensor and ultrasonic sensor mounted on the arm. The claws are used to grab the object. In order to avoid destroying objects during our tests, we used a sponge to simulate a delicate object. The touch sensor mounted above the claw would act as a sensor to decide when the object had been grabbed as well as if it too much pressure was being applied to the object or if the object was dropped.

The idea is that the touch sensor needs to be somewhat pressed in order for the robot to be aware that it has successfully gotten a hold of the object. However, if too much pressure is applied then the sponge would be squeezed excessively and the touch sensor would be pressed beyond a certain threshold indicating the object had been damaged.

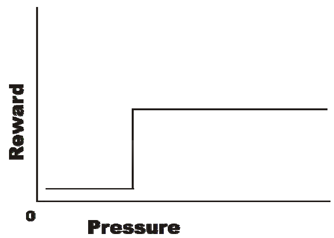

Figure 3. Pick-up Reward

Recall from our introduction that we have two competing rewards for a single state. This state represents the amount of pressure applied to an object to pick it up. One of the rewards would be a zero-one function, where if enough pressure were applied to the object, then it would be enough to pick the object up producing a reward of one. Before this threshold pressure is reached, this reward returns zero. Figure 3 illustrates this reward, which we will call the Pick-up Reward.

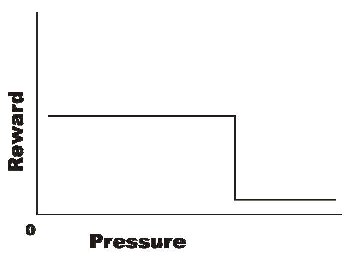

Figure 4. Not Crushed Reward

The competing reward also is dependent on the pressure state. It returns a value of one as long as pressure is below a certain breaking threshold. Once the pressure applied to the object exceeds that breaking threshold, the object is considered to have been damaged and a value of zero is returned. Figure 4 illustrates this reward, which we will call the Not Crushed Reward.

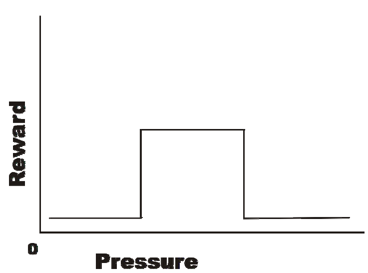

Figure 5. Combined Reward

The two competing rewards combined can be viewed as the function illustrated in figure 5. As pressure increases, zero reward is obtained until enough pressure is applied to pick up the object, then a reward of one is obtained. This reward of one is only obtained if concurrently not too much pressure is applied or the breaking threshold is reached and the reward returned is zero. The actual sponge object we used can be dropped as well. So if an insufficient amount of pressure is applied, then the sponge can be dropped, which we would consider a failed attempt.

Our objective during our experiments is to pick up the object as quickly as possible and return the arm to an initial start position. The goal of picking up an object as quickly as possible is directly affected by how careful the robotic arm must be at picking up this delicate object. The faster the object is picked up, the more likely it is damaged because greater pressure is generally needed to avoid the object from being dropped when it is being moved at faster speeds.

Theoretical Analysis

The key issue we are addressing is whether there is an advantage to using a combined reward structure in a single state (when it is natural to do so) or is it best to artificially separate the rewards into two separate states in order to fit the natural Reinforcement Learning model. In our service industry application, the single state of the pressure applied to the object we are attempting to pick up results in two rewards that somewhat oppose each other. Each reward is a natural direct result of the pressure state and thus should both be assigned during that state.

A combined reward structure for a single state intuitively requires a greater degree of computation and depending on the complexity of how the rewards should interact, this could slow down computation time significantly. However discretizing the rewards into separate states could also slow computation time. Recall from equation 3 of the background section on Reinforcement Learning that we need to solve an N x N matrix equation in order to compute value estimates during a learning phase. By splitting a single state into two states we actually increase the dimension size of our matrix to (N+1) x (N+1), also slowing computation time. The theoretical time to solve equation 3 is in the worst case $O(N^3)$. Thus the theoretical increase in time complexity with the added state would be:

$$(N+1)^3 - N^3 = 3N^2 + 3N + 1. \qquad (4)$$

Therefore, theoretically, if the state is only visited once per sampling estimate, then as long as the runtime for computing the more complex single state reward, R, is:

$$R(combined) < 3N^2 + 3N + 1 \qquad (5)$$

or $O(N^2)$, (i.e. the reward must run in quadratic time to the number of states or less) then the single combined state should be faster. However, if the state is visited N times per sampling estimate, the bound decreases to:

$$R(combined) < 3N + 3 + 1/N \quad (6)$$

or O(N), (i.e. the reward must run in linear time to the number of states or less). Note that these runtimes are based on a worst-case scenario of a fully connected network of states. The more sparsely connected the network of states, the lower this threshold would be.

In addition to the running time of the reward computation is the added possible advantage of using a function to compute our combined reward. Consider that the combined reward that takes into account multiple factors to produce its reward for its state could be the result of a complex interaction between the two or more rewards. If one were to discretize the rewards into separate states, the only way the rewards interact directly is through a discounting summation of equation 1. This means that they, at best, proportionately weight the two rewards and add them together as the most complex interaction when split into separate states. In contrast, a single state reward function could create a much more complex combined reward.

Experiments

In our experiments, we compared our combined reward in a single state to two other approaches. One alternative approach was to choose the state that assigned the Pick-up Reward first and then immediately follow that with a deterministic transition to the Not-Crushed reward state. However, if the Pick-up reward failed, then the robot immediately reset to try again during learning trials. The second alternative approach was to choose the Not-Crushed reward state first then immediately followed with the Pick-up Reward state but only if the Not-Crushed reward had not failed. We followed this approach since it seems intuitively obvious that if one fails to pick up the object, there is no point in testing if the object is crushed. Similarly, if the object was crushed, there is no need to check if the object was picked up.

We ran 12 trials where each trial allowed for 3 minutes of learning to find an optimal choice of speed and pressure to pick up our sponge object without crushing it. We recorded how many practice attempts were tried during each three minute learning phase. We also recorded the times each practice attempt took and whether they failed to pick up the sponge or crushed it. Finally for each trial we recorded an exploitation phase where the robot demonstrates the best-learned attempt to pick up the sponge.

Figure 6 illustrates graphically the time that it took the robot to pick up the object using the best learned approach in each trial. As can be seen graphically, the Combined Reward in a single state for our pressure value, has the greatest variability in terms of learned result. It not only produced the best-learned result (shortest time to successfully pick up the sponge without crushing it), but also the worst learned result (longest successful time) over our 12 trials. We tested a null hypothesis that the means of the learned trials for each approach were different from each other ($\mu_i \neq \mu_j$, where i and j represent our three different reward approaches, $i \neq j$). With 99% confidence interval, none of the means could be accepted as different. Thus we would accept that all three approaches on average produce comparable learned best pick-ups. But the variance of the Combined Reward method did significantly differ from the other approaches. Using an F distribution test on the variances, the Combined Reward approach has a 98% confidence that the variance differs from the variance of the other two approaches ($f_{ij} = 4.6$, $f_{ik} = 25.3$, where i is the Combine Reward approach, j is the Not Crushed Reward approach, and k is the Pick-up Reward approach).

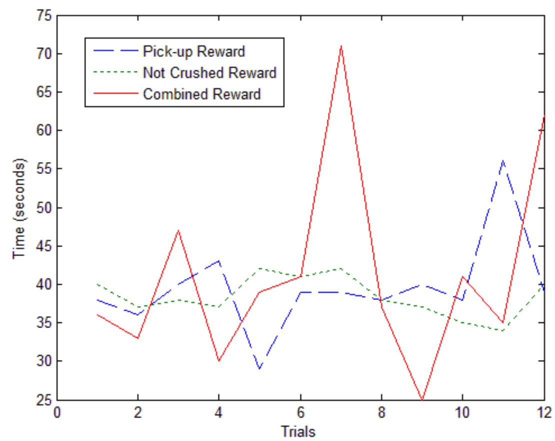

Figure 6: Time of Learned Pick-up

Looking at figure 6, the difference in variance implies that the Combined Reward approach tends to have the most variability in how well it learns. The reason for this wider variability is due to two factors at work during the Combined Reward approach. The first factor is that the Combined reward requires a two-threshold test, which takes slightly longer to compute, which can result in fewer practice trials in our 3-minute learning time. With fewer practice trials to learn from, this could lead to worse learned results. The second factor is that the more nuanced reward can give a better measure of value function, leading to better learned results.

What can be drawn from both our experimental results and our theoretical analysis, is that using a function that combines multiple factors to produce a combined reward can yield better learned results because the reward can take into account more complex relationships between the rewards than the simple weighting that would result in splitting rewards into separate states. But this benefit can be balanced out by the added computation time needed to produce this more complex reward. Thus, sufficient learning time is needed for the benefits of the more nuanced combined reward in a single state to be of benefit. The amount of actual time to compute the combined reward should not exceed $O(N^2)$, assuming a constant number of visits to the state per learning trial.

Conclusion

In this paper the researchers compared the traditional single state per reward approach with using a combined reward that incorporates at least two or more reward factors into a state. This combined reward allows for more subtle computations especially for reward factors that may oppose each other. By allowing for more complex computed reward structures, we may produce better learned results. We experimented on a practical implementation of this problem with a Lego robot that was charged with the task of learning to pick up a delicate object. The robot needed to apply sufficient pressure to pick up the object but not too much pressure or the object would be crushed.

In terms of theoretical results, we demonstrated that in the worst case, the combined reward should not exceed $O(N^2)$ computation time or the benefit in terms of efficiency would be outweighed by cost to compute the reward. However, this is a worst case scenario, and it is quite possible that the combined reward function must be significantly faster than $O(N^2)$ depending on the graph connectivity of the Reinforcement Learning model and the number of visits to the combined state.

From our robot experiments we demonstrated that the benefits of the more subtle combined reward can be outweighed by the extra time taken to compute the reward. In our experiments, it resulted in greater variability in terms of learned ability. Because we fixed the amount of learning time for our robot, the extra time needed to learn resulted in fewer practices to learn the task. These fewer practices competed with the benefit of the more subtle reward to cause greater variability in terms of performance for our learned task. Thus, for those considering using a complex function to compute rewards, they must take into account the amount of learning time allotted. If a sufficient amount of learning time is allowed, then the more subtle combined reward structure can produce better learned results. How much time should be allotted most likely is application dependent.

In terms of future work, we plan to expand on this investigation to explore a variety of possible reward functions with the goal of implementing them in a practical service robot.

References

[1] Sutton, R., & Barto, A. G., "Reinforcement Learning: An Introduction", MIT Press, Cambridge, Massachusetts, 1998.

[2] Burgard, W., Tranhanias, P., Hahnel, D., Moors, M., Schulz, D., Baltzakis, H., Argyros, A. “Tourbot and WebFair: Web-Operated Mobile Robots for TelePresence in Populated Exhibitions”, IEEE/RSJ Conf. IROS, 2002, pp. 77-89.

[3] Pollack, M. E., Engberg, S., Matthews, J.T., Thrun, S., Brown, L., Colbry, D., Orosz, C., Peintner, B., Ramakrishnan, S., Dunbar-Jacob, J., McCarthy, C., Montemerlo, M., Pineau, J., & Roy, N., “Pearl: A Mobile Robotic, Assistant for the Elderly”, AAAI Workshop on Automation as Eldercare, 2002.

[4] Krodel, M. & Kuhnert, K., "Reinforcement Learning to Drive a Car by Pattern Matching", Pattern Recognition: 24th DAGM Symposium. Springer Berlin/Heidelberg, 2002, pp 322-329.

[5] Lu, F, Patrascu, R., Schuurmans, D., “Investigating the Maximum Likelihood Alternative to TD(lambda)”, 19th International Conference on Machine Learning, 2002, pp 403-410.

[6] Michie, D., and Chambers, R. A., “BOXES: An experiment in adaptive control.” Machine Intelligence, Vol 2, 1968, pp 137-152.

[7] Barto, A. G., Sutton, R. S., and Anderson, C. W., “Neuronlike elements that can solve difficult learning control problems.” IEEE Transaction on Systems, Man, and Cybernetics. Vol 13, 1983, pp 535-549.

[8] Witten, I. H., “An adaptive optimal controller for discrete-time Markov environments”, Information and Control, 1977, Vol 34, pp 286-295.

[9] Watkins, C. J. C. H., “Learning from Delayed Rewards.” PhD. Thesis, Cambridge University, 1989.

[10] Lu, F., “Exploring Model-Based Methods for Reinforcement Learning”, PhD. Thesis, University of Waterloo, 2003.

[11] Sutton, R., “Learning to predict by the method of temporal differencing”, Machine Learning, Vol. 3, 1988, pp 9-44.

[12] Montemerlo, M., Pineau, J., Roy, N., Thrun, S., Verma, V., “Experiences with a Mobile Robotic Guide for the Elderly”, Proceedings of the AAAI National Conference on A.I., 2002, pp 587-592.

[13] Peters, J., Vijayakumar, S. and Schaal, S., “Reinforcement Learning for Humanoid Robotics.” Proceedings of the Third IEEE-RAS International Conference on Humanoid Robots, 2003, pp 1-20.

[14] Zhumatiy, V., Gomez, F., Hutter, M., Schmidhuber, J., “Metric State Space Reinforcement Learning for a Vision-Capable Mobile Robot.” Intelligent Autonomous Systems, 2006, pp 272 – 281.CASMED.

[15] Hansen, J., “Not eXactly C (NXC): Programmer’s Guide”, Version 1.0.1. b33, bricxcc.sourceforge.net, 2007.

Biographies

FLETCHER LU received Bachelor and Masters of Mathematics degrees from the University of Waterloo, Waterloo, Ontario, Canada, in 1997 and 1999 respectively, and a Ph.D. degree in Computer Science from the University of Waterloo, Waterloo, Ontario, Canada in 2003. Currently, he is an Assistant Professor of Health Sciences at University of Ontario Institute of Technology. His teaching and research areas include control systems, health informatics, machine learning, data mining, and fraud detection. Dr. Lu may be reached at fletcher.lu@uoit.ca

LORENA HARPER is a senior in the Department of Math and Computer Science at the University of Maryland Eastern Shore pursuing a Bachelors degree in Computer Science. Ms. Harper may be reached at laharper@umes.edu

DEVELOPMENT OF SAFETY EVENT METRICS FOR AN AVIATION ORGANIZATION

Anthony J. Morell, Purdue University; Mary E. Johnson, Purdue University; Edie K. Schmidt, Purdue University; Michael W. Suckow, Purdue University

Abstract

The introduction of safety management systems (SMS) to the aircraft services industry has stressed the importance of collecting and measuring safety event data to continuously improve management and operational processes. Aircraft maintenance companies provide services to the aviation industry. These companies have begun to collect safety event data and now recognize the need to prepare reports based on this data. While collecting information presents its own difficulties, this study focuses on analyzing safety data and presenting information to facilitate management decision making. This study has developed a set of metrics designed to analyze the safety event data and report it in an organized manner to include trends, control charts, Pareto charts, and aging analysis. Aviation managers assessed the usefulness of the set of metrics. This study has demonstrated that a set of useful metrics can be developed based on the safety event data to support everyday management decisions, as well as provide a foundation for further metric development.

Introduction

Aviation organizations have processes and procedures for collecting data, determining root causes, and recording the findings electronically in their safety event database system. The vast amount of information collected in company safety event databases needs to be distilled into a set of metrics in order for the data to be useful in decision-making. Within the Federal Aviation Administration's (FAA) advisory circular pertaining to safety management systems, it states, "Audits and other information-gathering activities are useful to management only if the information is distilled into a meaningful form and conclusions are drawn to form a bottom line" [1, p.19]. The International Air Transport Association (IATA) states, "To be useful, the data must be transformed into information that can be used by system managers to make informed decisions" [2, p. 4]. Without a useful set of metrics, management and technicians will not be able to identify and implement the proper improvements to processes and procedures.

This paper discusses the development of a set of useful metrics designed to support management decisions for system improvement. These metrics can be useful by providing up-to-date information regarding the safety event data that may be used by management to decide where improvement actions should be focused. The primary objective of the metrics developed was to provide useful information to support decisions made by management and to facilitate improvements in the system. An estimated 80 to 90 percent of contributing factors are under management control, while 10 to 20 percent are under the technician's control [3]. By analyzing the data and presenting a useful set of metrics, management has the ability to track and eliminate a large amount of the contributing factors that lead to errors, violations, and subsequent safety events within the workplace. Creating awareness and maximizing learning can be accomplished by sharing findings and recommendations with the affected employees [4]. Management can further reduce the remaining 10–20 percent of contributing factors that are under the technician's control by using these same metrics to increase awareness among the technicians and inspectors.

Review of Literature

A. Aviation Safety Management Systems

Transport Canada, the International Civil Aviation Organization (ICAO), and the Federal Aviation Administration (FAA) are all globally recognized for their contributions to aviation safety and safety management systems (SMS). In 2005, Transport Canada "placed the conceptual shifts involved in an SMS into the forefront of many airlines' agendas around the world" [5, p. 1]. ICAO's Safety Management Manual is intended to support the implementation of safety management systems [6]. The FAA advises a minimum standard for an aviation SMS [1]. The FAA's safety management standard is parallel to the framework developed by ICAO. The FAA issues and enforces regulations and minimum standards for safety in civil aviation. As of September 2008, the FAA does not require aviation service providers to implement an SMS, but in May 2008, the FAA recommended action to prepare for future implementations of SMS. Updates to FAA regulations may be found at www.faa.gov. Since aviation organizations are extremely safety-conscious, many are beginning to implement their own SMS, prior to a federal regulation requiring one.

A safety management system (SMS) has been defined as "an organized approach to managing safety, including the necessary organizational structures, accountabilities, policies and procedures" [7, p. 1–2]. An SMS is designed to "increase industry accountability, to instill a consistent and positive safety culture, and to help improve the safety performance of air operators. This approach represents a systematic, explicit, and comprehensive process for managing risks to safety" [8]. In three SMS documents [1, 7, 9], data collection and analysis are included as a valuable element of an SMS. Analyzing the data collected from an audit program, investigations, and employee reports allows an organization to be able to evaluate where improvements can be made to the organization's operational processes, as well as the SMS [1].

B. Investigation of Contributing Factors

The contributing factors to safety events are important to understand. Maintenance Error Decision Aid (MEDA) is an investigative process that was developed to determine contributing factors [10]. "The central philosophy of the MEDA process is that people do not make errors on purpose. While some errors do result from people engaging in behavior they know is risky, errors are often made in situations where the person is actually attempting to do the right thing. In fact, it is possible for others in the same situation to make the same mistake" [11, p. 17].

A large proportion of blame for errors has been traditionally placed on the technician because of the assumption that human error may be attributed to the actions of an individual and not because of the contributions of the environment in which the individual is operating [12]. Reason's Swiss Cheese model showed that events are not caused only by the last event, but that they are actually the end result of a long line of events of which the last act can be hazardous [13]. The MEDA tool was designed to take the investigator beyond the technician's active error and to explore as far up the causal chain as time and money would permit to correct the contributing factors [11].

C. Safety Metrics

The aviation industry strives for the same goal as any other industry—to reduce the number of events to zero. Measurements of safety performance allow a company to understand system performance and whether or not their safety processes are effective in reducing the amount of events [14]. Measurements may be used to help identify opportunities for improvement [15]. A sound measurement system supports decision making, indicates how the system is performing, helps in establishing priorities on important opportunities for improvement, and verifies that improvements are working [16]. Accident investigation is one area that should be monitored to ensure continuous improvement of the entire safety system [4]. Recommended measurements include percentages of types and causes of events and their location, average time from incident to investigation completed, and average time from investigation completed to corrective action implemented [4].

Allocating scarce resources is a challenge management faces on a daily basis. The Pareto chart is one way to make educated decisions based on data analysis. The Pareto concept, also known as the 80–20 rule, was developed by Vincent Pareto and has demonstrated that 20 percent of the known variables will account for 80 percent of the results [17]. Pareto charts may be used to identify the large problems that may be reduced more quickly and with greater impact, as opposed to focusing on eliminating small problems [18]. Using a Pareto chart, management can see the arrangement of data (errors, defects, or failures), view the most frequent deficiencies of a system, and eliminate or reduce these items as much as possible. Some researchers have adapted quality management practices to fit safety management's needs. In one such study, Pareto charts were used to indicate the frequency, severity, and location of problems in a facility [19]. This data was combined with perception survey data (proactive measures) to obtain a more complete view of what was occurring in the workplace [19].

Developing measurement systems is difficult, complex, and important [15]. When developing the set of metrics, the flow of the information through the system should also be addressed. Transport Canada [20] has documented the type of information that should be stored in such a database, as well as its path through the improvement process. The process highlights both reactive and proactive data flow into a database. Data should then be analyzed and the results communicated throughout the facility as part of a continuous system evaluation. System evaluation should be a continuous loop of information facilitating improvement to the SMS. In addition, measurements should be expected to change over time as conditions change [15]. By examining the literature, the authors defined the characteristics of useful metrics shown in Table 1.

Table 1. Characteristics of Useful Metrics

Easy to understand [10]
Supports decision making [2, 15]
Captures opportunities for improvement [1, 4, 15, 16]
Provides understanding of system performance [1, 14, 16]
Isolates important issues [16, 18]

Methodology

This paper presents the design and test of a set of useful metrics based on analysis of the types of safety event data stored in a typical aviation SMS. These metrics are designed to facilitate management decisions in the continual improvement of safety and operational procedures at an aviation organization. A four-step process was followed in the development of these metrics.

The first step was to understand what data is available. The data available in an SMS database largely determines what data can be presented or analyzed. Typical databases collect information on the date, type of incident, location of incident, and other data recommended by standard approaches, such as Boeing's MEDA [10, 11].

The second step was to develop the metric usefulness questionnaire. A questionnaire was developed to evaluate each metric for usefulness using questions based on the characteristics of useful metrics in Table 1. Scoring is based on a five-point Likert scale.

The third step was to develop the metrics. Using knowledge of aviation safety metrics and quality metrics, a set of metrics was developed using the data available in SMS databases. The metrics were selected based on those that had the potential to convey trends and provide other potentially useful information for management decisions.

The fourth and final step was to validate the usefulness of the metrics. The metrics developed in Step 3 were presented to eight management-level aircraft maintenance industry experts for evaluation. During the review of the metrics, these managers participated in a discussion and question/answer period. Finally, the experts were given an opportunity to voluntarily answer the questionnaire developed in Step 2 to evaluate the usefulness of the metrics. Participants, who were all from the same corporation, were instructed not to identify themselves on the questionnaires. The corporation had an active SMS policy, procedures, and database, but no set of metrics developed using the information available in the database.

Metric Development

From the literature and through multiple discussions with industry experts from the areas of quality, safety, and human factors, a total of eight metrics were chosen to support the decisions of managers and to drive system improvement efforts into the correct areas. The eight metrics are the aging of events, the number of events opened per month, the number of events closed per month, the number of days to respond to an event, the number of days to take corrective action, the frequency of each event type, the frequency of each severity level, and the frequency of causal factors.

The developed metrics were limited by the categories contained in the safety event database system. This section describes each of these metrics, what charts were used, and how the set of metrics can be used together to provide an illustration of the safety event data. No single metric is to be relied upon to describing the overall performance of the organization. As a group, these metrics provide insight into the information that may be presented by analyzing SMS data.

A. Aging Chart

An aging chart was selected to display the number of days that events have been open for all open events in the system. The chart is formatted as a histogram with boundaries set for five-day intervals, as seen in Figure 1.

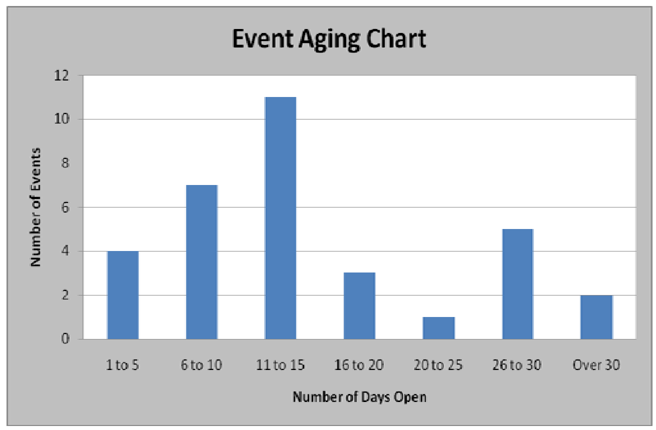

Figure 1. Event Aging Chart

This type of information is a valuable tool in identifying those events that have exceeded a time limit set by management. To develop an appropriate time limit, management will need to allocate appropriate resources to quickly resolve events and monitor the aging charts for a given period of time to determine where the standard should be set.

B. Events Opened/Closed per Month

Run charts and control charts were selected to provide information to managers regarding events opened and closed. These charts were selected for their applicability to processes that have variation due to both system causes and special causes. Separate run charts for the number of events opened each month and the number of events closed each month were developed. Using statistical techniques, these charts may be analyzed to provide evidence of any patterns within the discrete data, such as trends, oscillations, mixtures, and clustering. Examples of discrete data may include the number of complaints, the number of defects, or, in this case, the number of events opened per month, as shown in

Figure 2. The run chart may be set to display the number of events over specified time periods such as years, months, quarters, or weeks. This allows management to tailor the chart to the time period of interest. As more data is collected, the sophistication of analysis may also include statistical process control to identify common cause and special cause variation, to better understand and eliminate the causes.

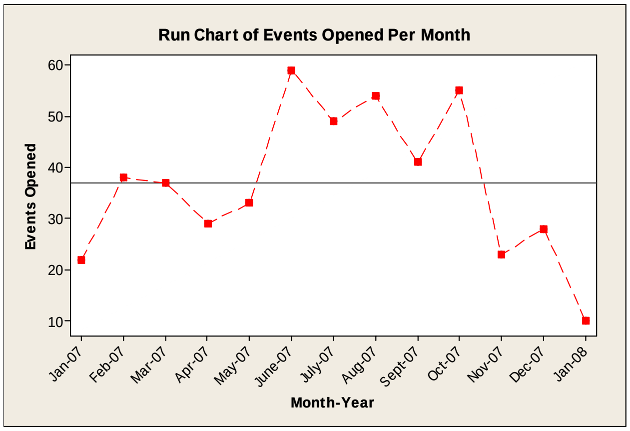

Figure 2. Run Chart of Events Opened Per Month

C. Response Time

Frequency histograms were selected for response time data presentation, as shown in Figure 3. Response time is defined as the number of days between the "Response due date" and the "Date response entered." A negative number represents a response that was entered before the due date, and therefore, completed early. A positive number means the response was late. The goal of this measurement is to provide managers with an average on how accurately an event response due date is being predicted. The information in these charts could be used to signal further investigation to provide insight into why events are not being responded to on time or what is causing the responses to be early. The response data is charted using a histogram.

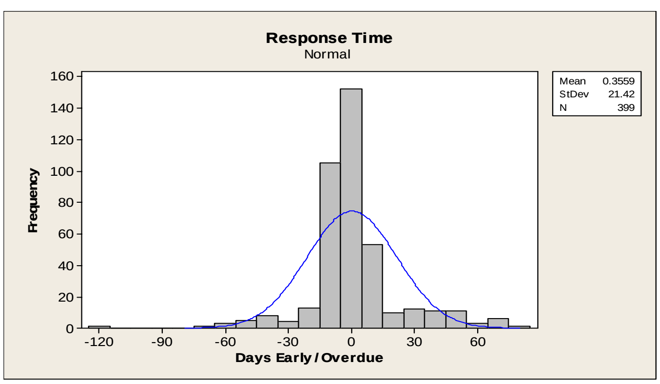

Figure 3. Response Time Histogram

D. Corrective Action Time

Frequency histograms were selected for corrective action time charts. These charts are similar in structure to those shown in Figure 3. Corrective action time is defined in this study as the number of days between the "Event Entered" date and the "Event Closed" date. Since an event can only be corrected in a positive amount of time, the charts produced will only indicate a positive number to the nearest day. In addition to displaying the distribution, the data may also be used to calculate other statistical measures such as average, median, and standard deviation. The data in these two charts is suitable for statistical process control charts. The management team chose to start their data analysis with frequency histograms, and to later move to more sophisticated statistical methods when the situation warrants it.

E. Frequency of Each Event Type

A Pareto chart was selected to display the frequency of each event type for a given month. This information is displayed by month in Figure 4. One could use the Pareto chart to identify the most frequent event type, and then investigate further by viewing the run charts or control charts for the same time period to better understand system performance. The event types can be charted over the entire time span of the database or by a given time period, such as months, years, or quarters, depending on the needs of management. Following the 80–20 rule, these charts identify the important few events to focus improvement efforts.

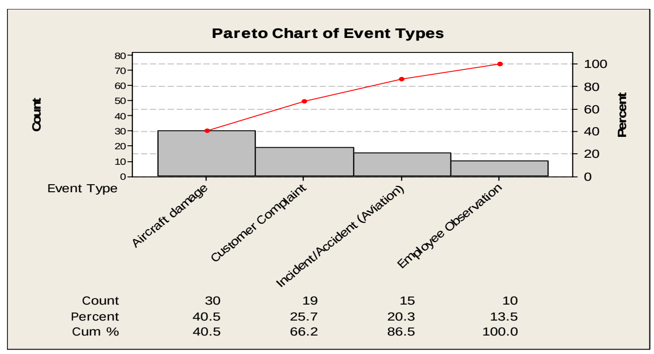

Figure 4. Pareto Chart of Event Types

The preceding six charts provide a general picture of the system. The remaining charts are meant to be used to gather additional information to clarify questions that may be raised during analysis of the preceding charts.

F. Frequency of Event Severity Levels

A Pareto chart was selected to provide more detailed information regarding the type of severity levels seen within the database over a certain time period, in this case per month. In Figure 5, the most severe level is “D,” while the least severe is “A.” Tying this chart to the Pareto for event types allows management to view the distribution of severity levels in relation to the events occurring during the same time period. Management should be careful not to ignore the most severe events just because they may be the least frequent. Events that are of severe levels should always be investigated.

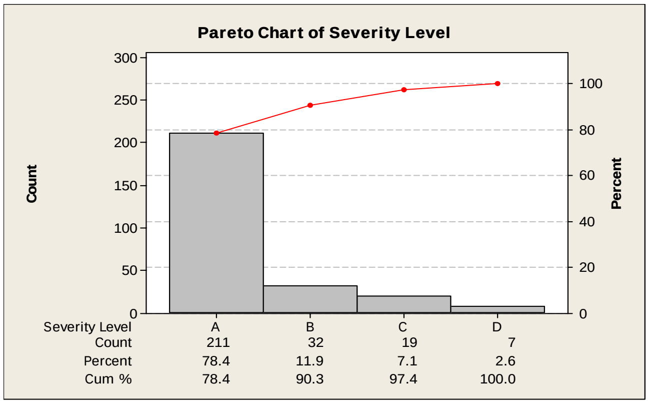

Figure 5. Pareto Chart of Severity Level

G. Frequency of Each Level of Causal Factors

A Pareto chart was selected to display the frequencies of the first two causal factor categories, similar to the chart in Figure 5. Investigations into root cause identify the causal factors for events. Each causal factor is comprised of three levels of categories: factor class, causal factor type, and response. The charts may be organized in a multitude of ways, depending on what is being investigated. In this study, the Pareto charts display the overall frequencies at each category level. Even at this level of granularity, management may begin to use these charts to understand which root causes are most common. This allows management to focus improvement efforts on the areas that may lead to greater improvements in a shorter period of time.

H. Combining the Metrics

When viewed independently, these charts provide information regarding measured aspects of the safety and quality systems. Though valuable as independent sources of information, the advantage of these metrics is that they may be used together to support management decisions. An out of control data point on statistical process control charts for events opened or closed per month can drive a manager to investigate the type of events, their severity levels, and what type of causal factors were found. Furthermore, the corrective action time and response accuracy can be tied in with the severity level and event type to determine why corrective action times and responses were at certain levels. The information discovered during these investigations can be used to improve processes, provide foundations for new standards, create new measurements, and aid in the development of new processes in the future. As SMS data becomes more prevalent due to future federal mandates, the need for analysis of the data becomes more pronounced as companies seek to gain insights into the system and to make informed decisions to improve safety management. A set of metrics provide more detailed information than a single metric.

Usefulness of Metrics

Once the analysis of the safety event data and the development of the metrics concluded, the metrics and sample charts were presented to a group of eight aviation industry experts. The experts represented management from areas including quality, safety, human factors, and information technology. These managers were of the level that had decision-making authority, understood SMS, and could allocate resources to resolve problems. During the presentation, the managers demonstrated keen interest in the metrics as they began to discuss ideas such as how to more specifically identify the categories of causal factors and event types in their SMS data collection.

A total of eight managers participated in the questionnaire. The questionnaire asked for a Likert scale rating from 1 (strongly disagree) to 5 (strongly agree) for seven statements:

1. The metrics were easy to understand.
2. I am able to make decisions supported by these metrics.
3. The metrics identify opportunities for improvement.
4. The metrics assist in displaying the level of system performance.
5. The metrics identify important issues.
6. I would use these metrics on a regular basis.
7. These metrics should be included in reports.

The results for each question were collected and are reported in aggregate. The overall mean score was 4.38, with a median of 4.5. Question 5 had the highest mean score at 4.63, while question 6 scored the lowest at 4. A score less than four was assigned by four respondents, three times for question 6 and once for question 2. Overall, these scores indicate that the respondents agreed that the metrics produced in this study contained useful information. Since the metrics produced in this study were the first set of metrics created for the SMS and seen by these managers, it is understandable if these managers may not immediately declare to use them on a regular basis.

Conclusions

International mandates for Safety Management Systems affect the entire aviation system, not just airlines or airports. Aviation service providers must also participate in SMS. While not US law as of September 2008, the FAA has SMS working groups and anticipates the mandate of SMS in US aviation in the near future. Currently, several aviation services companies collect SMS data, but perform little or no analysis of the data that may be used for decision-making. This study developed a set of useful SMS metrics through the review of previous literature in the areas of data collection, data analysis, and existing safety measures, as well as discussions with aviation industry experts. The outcome is a set of useful metrics that have already begun to support management decisions at one company who chose to adopt them. This study did not seek to develop a comprehensive set of company performance metrics. This study has provided a foundation for future research and development of safety event data analysis and metric systems.

The primary objective of the safety event metrics developed in this study was to provide useful information to management. These metrics are meant to support decisions made by management and to facilitate improvements in the system. During the presentation of the metrics to the group of industry experts, the usefulness of the metrics became apparent. During the presentation, the managers began discussing ideas of how to incorporate these metrics into more localized measures, such as scorecards for each work area. Based on the metrics presented, the managers also discussed how to gather more specific categories of causal factors and event types in their data collection.

The usefulness of the set of metrics developed in this study is supported by the results of a voluntary questionnaire. The experts who participated in the metric presentation were given an opportunity to answer the questionnaire and provide their opinion on the usefulness of the developed metrics. Respondents represented management from areas including quality, safety, human factors, and information technology. The results of the questionnaires confirm that this set of metrics is useful, and that the analysis of safety event data may be used to support management decisions.

The literature reviewed described the common elements of various safety management systems, how root causes are determined, and the characteristics of useful metrics. Based on the analysis of the safety event data and the results of the questionnaire, the data in a safety event database can be analyzed to produce useful metrics to support management decisions.

Recommendations

This paper assumes that organizations have taken the first step in developing useful metrics by collecting data from every safety event, regardless of the severity of the event. The developed metrics were determined to be useful according to a group of aviation experts who rely on information to make decisions. As aviation organizations begin to understand what type of data is useful and make necessary changes to their database systems, the organizations should continue to develop metrics to support decision-making.

By identifying the specific work area or product type, the data could be used to provide more specific information regarding safety events. This information could allow managers to pinpoint the events by focusing on a specific area of the facility. In addition to localizing events, placing specific weights on certain types of information could provide a more useful metric. One example would be to weigh the events per time period by the number of labor-hours expended. Labor-hours are a common measurement and are already collected by most aviation organizations. More detailed charts could be created for the aging charts, with specific aging charts for each event type or severity level. This could help management gain an understanding of the trends for each category and allow them to create a baseline for the amount of time an event should remain open.

As the metric systems are developed and improved for safety management systems, the addition of analyzing severity and risk of each event type could prove to be valuable. Severity and risk are already a category in many SMS databases. Any new metric should go through an approval process similar to this study's questionnaire. A questionnaire process should involve representatives of any group that will rely on the information if the metric is implemented. Creating a metric approval process to guarantee its usefulness will lead to a useful set of measurements, with each metric serving a purpose to the managers who will rely on the information to make decisions.

Acknowledgments

The authors are thankful to IAJC-IJME International Conference 2008 reviewers for their helpful and careful reviews.

References

[1] Federal Aviation Administration, "Introduction to safety management systems for air operators," *FAA Advisory Circular,* No. 120–92, 2006, Retrieved October 14, 2007,

http://rgl.faa.gov/Regulatory_and_Guidance_Library/rgAdvisoryCircular.nsf/0/6485143d5ec81aae8625719b0055c9e5/$FILE/AC%20120-92.pdf.

[2] IATA, "Global Aviation Safety Roadmap," 2007, Retrieved November 4, 2007, http://www.iata.org/NR/donlyres/D440B2E7-1DE8-4130-A796-F66BB5DDB451/0/GlobalAviationSafetyRoadmap.pdf.

[3] Boeing, "Maintenance Error Decision Aid," 2005, Retrieved October 1, 2007, http://www2.hf.faa.gov/opsManual/assets/pdfs/MEDA_guide.pdf.

[4] Petersen, D., *Measurement of Safety Performance*, Des Plaines, Ill: American Society of Safety Engineers, 2005.

[5] FSF Editorial Staff, "Unlocking the potential of a safety management system," *Flight Safety Digest*, Vol. 24, No. 11–12, 2005, pp. 1–15.

[6] ICAO, "Welcome to the safety management website," 2007, Retrieved December 5, 2007, http://www.icao.int/anb/safetymanagement/.

[7] ICAO, *Safety Management Manual*, 2006, Retrieved October 1, 2007, http://www.icao.int/icaonet/dcs/9859/9859_1ed_en.pdf.

[8] Transport Canada, "Regulatory amendments to improve aviation safety finalized," 2005, Retrieved December 3, 2007 http://www.tc.gc.ca/mediaroom/releases/nat/2005/05-h142e.htm.

[9] Transport Canada, "Components of the safety management system," CAR Part VII, Section 705.152, 2005, Retrieved December 4, 2007, http://www.tc.gc.ca/civilaviation/regserv/affairs/cars/part7/705.htm.

[10] Rankin, W., Hibit, R., Allen, J., and Sargent, R., "Development and evaluation of the maintenance error decision aid (MEDA) process," *International Journal of Industrial Ergonomics*, 26, 2000, pp. 261–276.

[11] Rankin, W., "MEDA Investigation Process," *Boeing Commercial Aero*, 2nd Quarter, 2007, Retrieved September 18, 2007, http://www.boeing.com/commercial/aeromagazine/articles/qtr_2_07/AERO_Q207_article3.pdf.

[12] Reason, J., *Human Error*, Cambridge University Press: New York, 1990.

[13] Reason, J., *Managing the Risks of Organizational Accidents*, Ashgate: Vermont, 1997.

[14] Toellner, J. "Improving safety and health performance: Identifying and measuring leading indicators," *Professional Safety*, Vol. 46, No. 9, 2001, pp. 42–47.

[15] Sink, D.S., "The role of measurement in achieving world class quality and productivity management," *Industrial Engineering*, Vol. 23, No. 6, 1991, pp. 23–28, 70.

[16] Sink, D.S., and Smith, G.L., "Reclaiming process measurement," *IIE Solutions*, Vol. 31, No. 2, 1999, pp. 41–46.

[17] Basile, F., "Great management ideas can work for you," *Indianapolis Business Journal*, Vol. 16, 1996, pp. 53–54.

[18] Eckes, G., *The Six Sigma Revolution: How General Electric and Others Turned Process into Profits*, New York: John Wiley, 2001, p. 85.

[19] Williamsen, M.M., "Six Sigma safety: Applying quality management principles to foster a zero-injury safety culture," *Professional Safety*, Vol. 50, No. 6, 2005, pp. 41–49.

[20] Transport Canada, "Safety management systems for flight operations and aircraft maintenance organizations (TP 13881E)," 2002, Retrieved October 13, 2007, http://www.tc.gc.ca/publications/EN/TP13881/PDF%5CHR/TP13881E.PDF.

Biographies

ANTHONY J. MORELL was a graduate student in the Aviation Technology department at Purdue University. His BS and MS degrees are from Purdue University. Mr. Morell may be reached at anthony.morell@gmail.com

MARY E. JOHNSON is an Associate Professor in the Aviation Technology department and the Industrial Technology department at Purdue University. She is interested in performance measurement and improvement and the incorporation of creativity in the learning process. Her PhD is in Industrial Engineering from The University of Texas at Arlington. She may be reached at mejohnson@purdue.edu

EDIE K. SCHMIDT is an Associate Professor in the Industrial Technology department at Purdue University, where she conducts research in supply chain, distribution, and project management. Her PhD is from Purdue University. Dr. Schmidt may be reached at schmidte@purdue.edu

MICHAEL W. SUCKOW is an Assistant Professor in the Aviation Technology department at Purdue University. He is a pilot with extensive airline experience prior to joining Purdue. He may be reached at msuckow@purdue.edu

ENHANCEMENT TO THE CONDITIONED HEAD TURN TECHNIQUE TO MEASURE INFANT RESPONSE TO AUDITORY STIMULUS

Barry A. Hoy, Devry University; Eleanor L. Hoy, Norfolk State University

Abstract

A phonetic recognition and reaction measuring tool is presently in use by sociological and psychological researchers at the University of Washington. The tool makes use of a system known as the Head Turn Technique (HTT). The tool measures the test participant's response to subtle changes in phonetics he or she is hearing by sensing the movement of the participant's attention focus toward the source of the phonetic stimulus. The existing tool has been largely unchanged for five years and may benefit from a technological revision. The tool, as it is, relies heavily upon human interface, which may be contributing to inaccuracy of measurement and limitations in the types and richness of data that are captured. In the existing process, a test administrator manually initiates the event prompting the change in the focus of the subject's attention. The occurrence or non-occurrence of the response is then judged by the test administrator. Computer control is limited to the generation of the phonetic stimulus. The proposed revision includes a laser pointing device and a laser light receptor array, software modification, and revision of the test procedure. The enhancement could add the ability not only to detect the occurrence of the head turn event but also to time various aspects of the event. Computer software would trace the path of the laser pointer's beam as the head is moved and hence the precision with which the head is moved. It could also measure the divergence between the orientation of the head and the focus of attention.

Introduction

The present iteration of the HTT test process was developed for use in measuring infant and toddler response to subtle changes in the phonetic composition of sounds to which the child is being exposed [1, 2]. Figure 1 presents a plan of the test layout showing one of the team members and the test participant. Figure 1 does not show the second test team member, since that member is not present at the test location but administers the test from a remote location. As can be seen by examination of Figure 1, the toy waver is situated approximately 30 to 45 degrees to the participant's right, while the loudspeaker and display are 30 to 45 degrees to the participant's left.

Related Research

The process presently includes two test team members in addition to the test participant. The team is comprised of the test administrator and the toy waver. The test administrator's function is to manipulate the computer that is in control of the generation of the phonetic stream and to record the response of the participant. The phonetic stream is composed of a sequence of phonetic sounds that are presented as single syllables to the participant through a loudspeaker. In the sequence, a phonetic is repeated several times. At a given point in the sequence, the phonetic undergoes a subtle change hereinafter known as a phonetic change event. As an example, the phonetic "Lah" may be repeated until the test administrator initiates the phonetic change event. At this point, the phonetic "Bah" is repeated three times. This phonetic sequence may be better understood by examining Figure 5. The goal of the test is to measure the participant's reaction to the phonetic change event. Participant gaze reorientation, coincident with the phonetic change event toward the speaker from which the sounds are emanating, is recorded by the test administrator as a successful detection by the participant that a phonetic change event has occurred.

The toy waver's function is to attract and maintain the attention of the participant by use of actions and gestures with the toy. In addition to these two members, the parent of the infant or toddler participant may be present to reduce tension in the participant. The test administrator is not visible to the toy waver, the participant, or the parent of the participant. In this way, neither the toy waver nor the parent will know when the phonetic change event will take place. This is important, since such pre-awareness might prompt the parent or toy waver to anticipate the movement of the participant's head with an inadvertent glance in the direction of the loudspeaker. Such actions have been demonstrated to be sensed by participants, a phenomenon referred to as gaze following [3]. Such gaze following would create an undesired control variable that would have a contaminating effect on the outcome of the test.

Test participants are males or females not younger than the age of six months. In the present test process, the infant or toddler participant is placed in the parent's lap in close proximity to the toy waver and to the loudspeaker and display. The toy waver maintains the concentration of the participant by showing the participant a toy, generally a stuffed animal. Simultaneously, the computer software used to administer the test causes an audible repetition of a syllable which is common in the English language. An example is "Lah." The phonetic "Lah" is repeated at a rate of approximately once per two seconds. At an appropriate moment, the test administrator, through computer control, initiates the phonetic change event, at which point the repeated phonetic changes from "Lah" to another phonetic, "Bah," for example. The changed sound is repeated three times, and then the software reverts back to the original phonetic. With the change in the phonetic, the display that is on the same axis as the loudspeaker will present a picture of a stuffed animal. In this way the participant is presented with a pleasing stimulus as a reward for having noticed a change in the syllable that is being repeated.

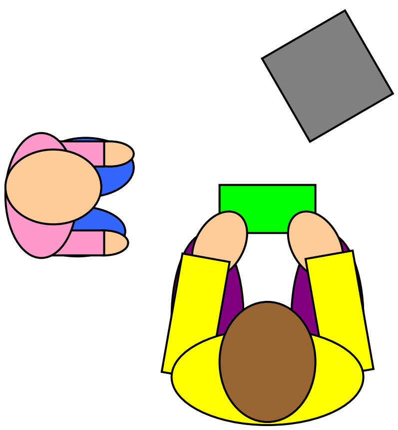

Figure 1. Plan of Test Process Layout

As depicted in Figure 2, the function of the toy waver is to maintain the concentration of the participant for the duration of the test. In this figure, the child's attention is being attracted by the toy waver, and the focus of the child's gaze reflects the child's attention to the toy waver's activities [4]. This referent attention associated with gaze has been demonstrated in infants as young as six months [5]. The child's gaze is fixed upon the toy, and the head position reflects the attention of the child. While the child is watching the toy waver, the loudspeaker emits the repeated phonetic: "…Lah…Lah…Lah…"

When the test administrator is confident that the child's attention is properly fixed on the toy, he or she initiates the phonetic change event. Simultaneous with this change in the phonetic, the monitor presents an image of a stuffed animal similar to the one held by the toy waver. The initiation of this image is delayed slightly so that it is clear that the change in the participant's focus of attention was caused by the change in sound and not by the occurrence of the image on the display.

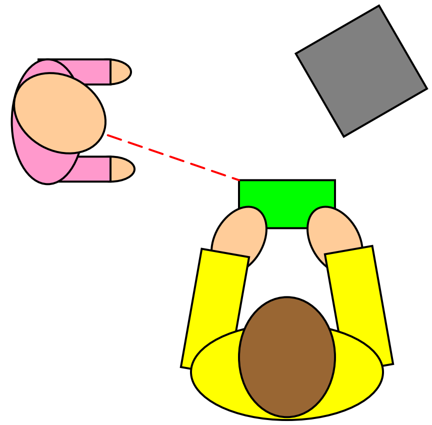

Figure 2. Participant's Gaze and Attention Focused on the Toy

The participant's attention shifts to the loudspeaker and display at the moment that the participant senses the phonetic change event. This realignment of the attention axis or the absence of same is observed by the test administrator. Successful detection of the phonetic change is indicated by a shift in the participant's gaze toward the loudspeaker and display as depicted in Figure 3. This reorientation of gaze in known as the head turn event.

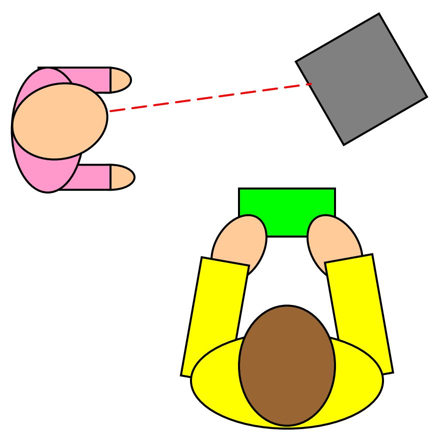

Figure 3. Participant's Gaze and Attention Focused on the Display

It is up to the test administrator to record that the head turn event has been executed. The test administrator records occurrence or nonoccurrence only. There is no ability to fix in time the occurrence of the phonetic change event or the head turn event.

Enhancements to Existing System

This conceptual article presents a revision of the HTT. The revision could enhance observations in four ways:
1. It has the potential to provide the ability to measure the time interval between the phonetic change event and the beginning of the head turn event.
2. It has the potential to measure the time interval between the beginning of the head turn event and the end of the head turn event. (These two intervals are summed to produce the total time interval between initiation of the phonetic change event and the completion of the head turn event.)
3.It has the potential to trace and store the path of head pointing during the head turn sequence.
4. It has the potential to measure the divergence between the orientation of the head and the focus of attention.

The revision makes use of a system that permits accurate measurement of the orientation of the head as well as timing of the head turn test sequence. It embodies two hardware elements not in use in the present system design. These hardware elements include a laser pointing device (LPD) embedded in a cap that is worn by the participant and a laser receptor array (LRA), which detects the direction in which the LPD is oriented and then generates two binary numbers corresponding to that direction. The first binary number corresponds to the horizontal orientation, while the second number corresponds to the vertical orientation. The enhancement also embodies a software element that converts the binary number generated by the LRA to a virtual location, which is stored by the administrator's computer and which is presented on the monitor that the administrator is using. These revisions necessitate several procedural additions and modifications to the test procedure.

Laser Pointing Device (LPD)

The infant and/or toddler participant will wear a knitted or similar cap to which an LPD is fixed. Such devices are available at minimal cost. They are small and light. The most difficult aspect of LPD design is its packaging and mounting. An LPD resembles a shorter version of an instructor's laser pointer. Such a device will be mounted to the participant's cap. Since the device is small in size and light in weight and since infants and toddlers are accustomed to wearing caps, it is anticipated that the LPD will create no distraction to the participant. It is well known that such devices emit a finely focused light in the visible spectrum, a bright red dot. This red dot might serve to distract the participant if it is visible to the participant. To overcome this shortcoming, it is proposed that the LPD be oriented rearward so that its emitted light is out of the field of view of the participant.

Laser Receptor Array (LRA)

The second hardware addition is the LRA. Such an array resembles a segment of the surface of a sphere that measures 60 degrees vertical by 120 degrees horizontal. The complete sphere has a diameter of 2–3 meters. On this surface are mounted multiple receptor elements in a square matrix or square grid. The distance between elements (element density) is dictated by the beam width of the laser emitter and the desired resolution of the path measurement discussed below. In the present configuration, the participant is held on the parent's lap. Since the laser is directed rearward, the presence of the parent behind the participant's head would block the laser; consequently, under the revised design, the parent will not be present at the test location. As shown in Figure 4, nothing can be interposed between the participant and the LRA; consequently, the participant may not sit on the parent's lap.

The distance between the participant and the LRA is anticipated to be between 1–1.5 meters. The shape and size of the LRA must be such that an element is available to be illuminated by the LPD at all potential orientations of the head of the participant regardless of the attention source. The function of the array is to create two binary numbers for processing by the software routine that is resident in the administrator's computer. As revealed previously, the two numbers will be generated by the array based upon which element is illuminated in the horizontal and the vertical axis. The representative binary numbers will be transferred to the computer that is being used to control the test. The layout of the revision is presented in Figure 4.

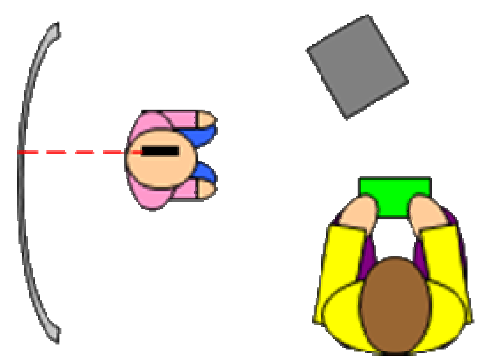

Figure 4. Revised Test System Layout

Software

In the existing test configuration, the software is used to initiate the change in phonetics. Under the revision, it is necessary to modify this software so as to add several capabilities, as follows:

1.The revised software must embody a graphic user interface (GUI) that serves as a "dashboard" for the test administrator. This dashboard must give the administrator control over those functions necessary to perform the test, store the results, display the test as it occurs, replay the test, and mathematically analyze the test from a time/event standpoint.
2. The revised software must be able to receive and process the binary numbers from the LRA to display the orientation of the laser dot on the computer monitor and to store that location in memory.
3. The revised software must be capable of executing all of the existing functions plus all of the additional functions of the revised test procedure. These functions include phonetic change event initiation, graphic presentation of the orientation and movement of the head in the appropriate format, control of the phonetic that is broadcast via the loudspeaker, control of the presentation of the toy on the participant's monitor, storage of data that is captured during the test, replay of stored test results, and the ability to process test results such that the beginning and end of the head turn event can be established.

Capturing the Head Turn Event

As a starting point on software and GUI development, the ability to capture the time measured in seconds at which the phonetic change event occurs is proposed. This time event (designated "T1") will begin the time interval measurement sequence. The occurrence of the phonetic change initiation will start a timer within the software. Resolution of the timer should be at least three decimal places, providing the ability to measure time with an accuracy of .001 second. A time designation "T2" will be given to the time at which the orientation of the head begins its excursion from its initial position (focused on the toy waver's activity) to its new attention. Finally, the designation "T3" is given to the time at which the head is fixed at its terminal position (focused on the loudspeaker and monitor). Figure 5 may be examined to provide a better understanding of the time sequence.

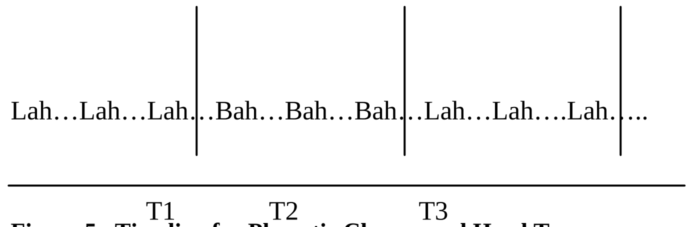

Figure 5. Timeline for Phonetic Change and Head Turn Occurrence

In the interest of clarity, the following explanation is presented. As the test sequence begins, the test administrator will direct the toy waver to begin the activities that are intended to hold the attention of the test participant. The participant's attention, indicated by gaze, will focus on the toy and toy waver. The control computer will direct a phonetic syllable to the loudspeaker. The software must have the ability to record the output of the LRA, which will indicate that the participant is paying attention to the toy and toy waver. When the administrator is satisfied that the attention of the participant is attracted to the toy, the administrator will initiate the phonetic change event. The software must have the ability to designate this time as "T1." The control computer will then direct the new phonetic syllable to the loudspeaker.

As the participant senses the change in phonetic, his or her gaze will begin to reorient toward the loudspeaker and display. The head will begin to shift, reflecting that the participant is intending to shift his or her gaze in the direction of the loudspeaker and display. The test software will sense this change in gaze orientation predicated by a change in the binary numbers that are created by the LRA. The test software routine will designate the instant in time at which the head began to move as "T2."

The participant's head will continue to move until it has become fully reoriented in the direction of the loudspeaker and display, at which point it will stop. The output of the LRA will generate two binary numbers that indicate the new head orientation. These numbers will be processed by the control software routine, which will designate the time at which the head stopped as "T3."

As the head moves from its initial to its terminal position, the LPD will illuminate and activate elements in the array that capture the instantaneous orientation of the head. The LRA will output binary numbers, which will be sent to the control computer for processing in the control software. A subroutine within that software will map this path and display the path on a two-dimensional grid that is part of the GUI, as shown in Figure 6. This map or path will essentially be a history of the participant's head movement for the duration of the test. The subroutine will also have the power to store the history of the head movement for statistical processing and for the purpose of replay.

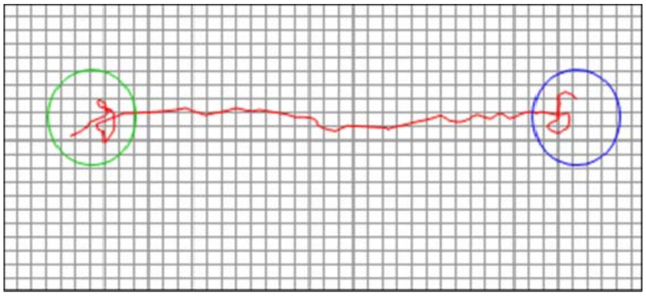

Figure 6. Notional Map or Path as Displayed on the Control Computer as Part of the GUI

Test Format

Post-revision, the control of the entire test process will be relinquished to the computer and software. The action by the test administrator will be simply to initiate the test immediately after the attention of the participant is focused on the toy waver. Occurrence or non-occurrence of the head turn event would be sensed by the computer and software as it establishes the occurrence of T1, T2, and T3.

Calibration Sequence

As the participant's gaze is focused on the toy waver, his or her head is oriented toward the toy. Hence, the LRA elements that are being illuminated are expected to fall within a specific area, which is designated the rest gaze axis area of uncertainty (RGAAU). As the participant's gaze shifts to the loudspeaker and display, the head orientation will also shift, illuminating LRA elements that are within a stimulated gaze axis area of uncertainty (SGAAU). Owing to differences in each participant's muscular coordination, it may be necessary to recalibrate the test system with each new participant. A young participant with a poorly developed ability to hold his or her head still while gazing at an object would be expected to illuminate LRA elements over a relatively large area. On the other hand, an older participant with better muscular control might be expected to hold his or her head relatively still while looking at the object. In the case of the older participant, the area of illumination would be expected to be smaller than for a younger infant.

The beginning of the head turn event is established as the head begins to turn in the direction of the loudspeaker. This motion results in an LRA element being activated that is outside of the area within which all element activations indicate that the participant's head is oriented toward the toy waver. The reader's attention is invited to Figure 6. For purpose of clarity, the beginning of the head turn event (T2) would be established at the time when the red path moves outside of the green circle designating the RGAAU. The software would be written such that it detects the instant at which this occurs and stores the time of occurrence. The end of the head turn event (T3) is determined to occur at a time after T2 when all subsequent element activations occur within the SGAAU, the blue circle on Figure 6. The borders of these areas of uncertainty must be precisely determined to determine with precision the times of occurrences of T2 and T3. As discussed above, the location and dimensions of these areas of uncertainty would be expected to be different from one participant to the next. Consequently, the test system would need to embody a calibration mode intended to determine the location and dimension of these areas of uncertainty before the test is conducted.

The calibration procedure would be executed by the test administrator before each test. A notional calibration procedure is as follows:

1. Participant takes his or her place within the test position with cap on and LPD energized.
2. Toy waver attracts the attention of the participant to invite attention to the initial position.
3. Position of the head as detected by array element illumination and presented on the control computer monitor is noted by the test administrator. (It is anticipated that multiple elements will be illuminated owing to lapses in muscle control creating inadvertent movements of the head, in spite of the fact that the focus of attention has not changed. The software modification making use of the map discussed above would give the test administrator the ability to place a circle around all element illuminations on the monitor by use of the mouse cursor. The child's gaze will focus on toy waver activity. The circle provided will declare the RGAAU. At the initiation of T1 during the actual test, the head will move outside of this circle as it begins its excursion to the new attention source. After T1, two subsequent element illuminations outside of this circle will be recognized by test software as T2 during the actual test.)
4. The test administrator initiates an audible event that invites the attention of the participant to the loudspeaker and display axis.
5. Repeat step 3. The circle provided as described above is declared to be the SGAAU. Two subsequent illuminations of elements within this circle during the test will be recognized by the software as T3.

Potential Angular Accuracy

Angular accuracy is imparted by the number, position, and density of the elements in the LRA. The maximum number of elements will be established by the size of the footprint of the laser emission as it strikes the array and the size of the receptor elements. The LPD may be assumed to have a beam width that will not exceed 0.3 degrees, which is typical for the emitters used in such devices. It is anticipated that the distance from the head of the participant to the surface of the array should be on the order of 1–1.5 meters so that the array may be kept to a manageable size. At this distance, the footprint of the laser illumination is roughly 3–5 mm.

It is unlikely that orientation measurements will need to be accurate to less than one degree on either axis. More likely, 3–5-degree accuracy will be more than sufficient. At 1 meter away, the separation of receptor elements will need to be 52 mm to provide 3-degree resolution. It is further anticipated that the head position will need to be measured in a predominantly horizontal axis. As the participant turns his or her head from RGAAU to SGAAU, the head could be expected to traverse a horizontal arc described by 60 degrees. To permit the capture of element illumination produced as the head overshoots and then corrects, the array should go beyond the 60-degree arc by an additional 30 degrees in both directions. The total horizontal span of the array must therefore be 120 degrees. The array should also permit the capture of information as the head moves off axis in the vertical direction. This means that the array must permit element illumination 30 degrees above and below horizontal for a total vertical arc of 60 degrees. Given the 3-degree resolution requirement, such an array will contain 800 receptor elements. Higher element density provides additional accuracy in the angular measurement.

Considering the physical and optical parameters of the LPD and the individual receptor elements, it may be necessary to defocus the LPD to broaden the footprint. In this way, the likelihood that no element is illuminated by the LPD because of the wide space between receptor elements can be minimized.

Potential Time Accuracy

Time accuracy is a function of the parameters established in the subroutine that initiates the test and captures the position data from the LRA. Time accuracy resolution must be sufficient to capture the activation of each of the receptors as they are illuminated. Angular rotation of the head of the participant can be expected to be as high as 300 degrees per second for the time during which the head is in motion from its initial position to its new position. This means that a 60-degree movement can be executed in 200 milliseconds. It is unlikely that head motion in participants will exceed this rate. During that time, the LPD will have illuminated not less than 20 receptor elements. Therefore, test software must be able to capture 100 receptor activations per second. For this reason, a minimum of three digits to the right of the decimal point are needed to capture all receptor activation events.

Next Research Phases

The disciplines involved in this project include electronic engineering technology, computer engineering technology, software engineering, sociology, and medicine. As has been stated, the LRA must be constructed. Conceptually, this array makes use of a fairly simple photo transistor coupled to a binary number generator. Any undergraduate or graduate electronic engineering or technology program would contain the expertise to develop, construct, test, and produce this array. The LRA produces a binary number which represents the elements that have been activated by the LPD. This number is sent to the control computer and processed by the software that is resident in that computer. Again, an undergraduate computer engineering program would contain the expertise required to develop the interface between the LRA and the control computer. Development of the software might be the most complex task in the implementation of the system. This task may best be executed in a graduate-level software design program.

While the system design and implementation invokes technical or engineering disciplines, its employment is clearly within the disciplines of medicine or sociology. The graduate program at Washington University, in which the foundations of the concept were initially laid, can be observed as establishing the parameters of such programs.

Summary and Implications

As can be seen, the revision to the existing test provides the ability to measure the speed with which the participant is able to process the perception of an audible stimulus and convert it to a completed head turn response. For the concept to be valid, some measure of accuracy must be part of the measurement. This need for accuracy is predicated upon the idea that head position is an accurate indicator of focus of attention. This need not be assumed, since Caron, Butler, and Brooks [4] demonstrated the relationship at least in infants that have reached the age of 12 months. Parenthetically, the revision to the HTT might facilitate the measurements suggested by Caron et al. in younger infants. Since a connection has been established between certain pathologies and impairment of the head turn function [6], the measurement of these times can be a useful diagnostic tool for identifying conditions that impact such times, choosing therapies intended to remediate such conditions and longitudinally testing the success of those therapies when applied. The hereditary connection examined by other researchers [7] could also be further explored.

There is cross-sectional value in determining the impact of various environmental factors upon such measurements. It may be inferred that the interval T1 to T2 is useful in measuring mental processing time, while the interval T2 to T3 is an indicator of muscle control and optical/auditory performance. The impact of a wide array of factors upon these times could be tested.

This technique could be applied in the Freiberg and Crassini [8] examination of infant sensitivity to Sound Power Level (SPL). Minor adaptations that could be implemented by the tester are all that are required. The Hollich, Newman, and Jusczyk [9] inquiry into an infant's ability to synchronize visual and audible stimuli might enjoy a new dimension. The study conducted by Liu, Kuhl, and Tsoa [1] could be expanded to measure not only the basic response to the audible stimulus but the speed with which the response is executed. Additional potential applications of the test are numerous.

References

[1] Liu, H.M., Kuhl, P.K., and Tsoa, F.M., "An Association Between Mother's Speech Clarity and Infant's Speech Discrimination Skills," *Developmental Science*, Vol 6, No. 3, 2003, pp. 1–1031.

[2] Anderson, J.L., Morgan, J.L., and White, K.S., "A Statistical Basis for Speech Sound Discrimination." *Language and Speech*, 2003, Vol. 46, No. 2/3, pp. 155–183.

[3] Brooks, R. and Meltzoff, A.N., "The Importance of Eyes: How Infants Interpret Adult Looking Behavior." *Developmental Psychology*, Vol. 38, No. 6, pp. 958–966.

[4] Caron, A.J., Butler, S., and Brooks, R., "Gaze Following at 12 and 14 Months: Do the Eyes Matter?" *British Journal of Developmental Psychology*, Vol 20, No. 2, 2002, pp. 225–240.

[5] Bortfeld, A.A., Morgan, J., Golinkoff, R.M., and Rathburn, K., "Mommy and Me," *Psychological Science*, April, 2005, Vol. 16, No. 4, pp. 298–304.

[6] Benasich, A.A., "Impaired Processing of Brief, Rapidly Presented Auditory Cues in Infants With a Family History of Autoimmune Disorder," *Developmental Neuropsychology*, 2002, Vol. 22 No. 1, pp. 351–372.

[7] Choudhury, N., Leppanen, P.H.T., Leevers, H.J., and Benasich, A.A. "Infant Information Processing and Family History of Specific Language Impairment: Converging Evidence for RAP Deficits from Two Paradigms," *Developmental Science*, Mar 2007, Vol. 10, No. 2, pp. 213–236.

[8] Freiberg, K. and Crassini, B., "Use of an Auditory Looming Task to Ttest Infants' Sensitivity to Sound Pressure Level as an Auditory Distance Cue," *British Journal of Developmental Psychology*, 2002, Vol.19, No. 1, pp. 1–10.

[9] Hollich, G., Newman, R., and Jusczyk, P.W., "Infants' Use of Synchronous Visual Information to Separate Streams of Speech," *Child Development*, 2005, Vol. 77, No. 3, pp. 598–614.

Biographies

BARRY A. HOY, PH. D. is the Academic Chair of Electronic and Computer Technology at DeVry University. He is part owner of Pairodocs Training and Development. Dr. Hoy is a retired Naval Officer in the electronics field and has more than 17 years of experience as an educator, corporate training director, and educational systems developer. Dr. Hoy can be reached at bhoy@devry.edu

ELEANOR L. HOY, PH. D. is an electronics instructor at Norfolk State University. She is part owner of Pairodocs Training and Development. Dr. Hoy has more than 25 years of experience in the electronics field as a journeyman, foreman, and educator. Dr. Hoy can be reached at elhoy@nsu.edu

SOFTWARE REVIEW
KICAD FOR SCHEMATIC CAPTURE AND P.C. BOARD LAYOUT

Reviewed by Jonathan M. Hill, University of Hartford

Introduction

KiCad is software for the creation of electronic schematic diagrams and printed circuit board artwork. It is useful for everybody working in electronic design, supporting the design of printed circuit boards with up to 16 copper layers. KiCad runs on GNU/Linux and MS Windows. It is occasionally tested on various versions of UNIX, especially FreeBSD and Solaris, and there are unofficial binaries for Macintosh. I primarily run KiCad on Windows Vista, as well as Windows XP.

For my research, I primarily develop relatively simple adapter cards for use with commercially manufactured off-the-shelf development boards. As an educator, I am responsible for providing students with electronic CAD software for use in their projects. KiCad is ideal in both cases. After researching the product on the Web, I notice that others use KiCad in more sophisticated designs such as embedded microprocessor systems.

The package is comprised of the following programs. The project manager, also named KiCad, organizes files in a project and launches the remaining tools:

KiCad – Project manager
Eeschema – Schematic capture tool
Cvpcb – Component selector tools
Pcbnew – P.C. board layout tool
Gerbview – Gerber file viewer tool

Many of the tools include additional attendant software. The schematic capture tool and the P.C. board layout tool each have its own editor for creating or modifying schematic symbols and the corresponding artwork, respectively. The layout tool also includes auto-router software.

Using KiCad

To begin, first create a new project. Next, produce schematics. The component selector is used to match schematic symbols with the corresponding artwork or footprint. The layout tool produces industry standard Gerber files and drill files so that you are free to choose a board manufacturer. The artwork can be viewed in two or three dimensions.

Figure 11 is the schematic capture tool. With buttons along three sides of a window, the tools are neatly organized and uncluttered. Pop-up hints describe the function of each button. There is also an undo feature.

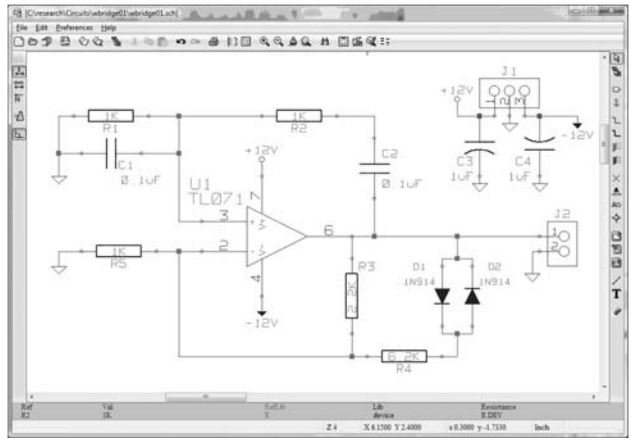

Figure 1. Schematic capture

The pull-down menus are neatly organized and easy to understand. As shown in Figure , the final layout can be rendered in three dimensions. A companion program called Wings3D, not reviewed here, can also be used to produce 3D artwork.

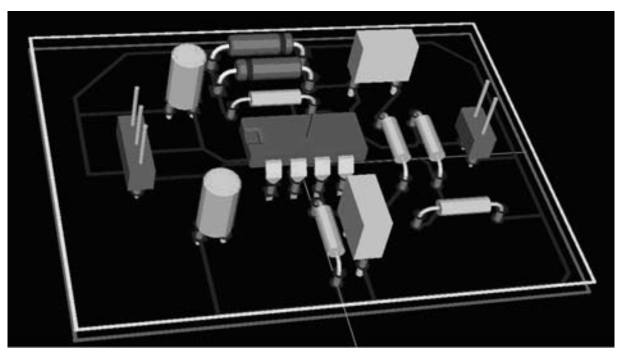
Figure 2. Layout display in 3D

A pull down menu provides a list of short-cuts or hot-keys. By using a simple configuration file, hot-keys can be reassigned either on a system or per-user basis. Installing KiCad on Windows is performed by running a self-installing executable file.

Without getting into detail, the essence of free software is the community of its users and developers. The developers are at the core of the user community. As a user, you are a member of this community, and you can also become involved. When considering any free software, look for the community of users and developers and examine the content they provide. A quick Internet search of KiCad provides a variety of information. For those new to electronic CAD, there are tutorials. For experts, the documentation provided is decent. There are discussion groups and Web sites with KiCad libraries and various utilities. In a nutshell, KiCad is well supported by those involved.

KiCad is designed and written by Jean-Pierre Charras, a researcher at GIPSA-lab (Grenoble Image Parole Signal Automatique laboratory) and a teacher in the field of electrical engineering and image processing at IUT de Saint Martin d'Hères in France. While the package name appears in several forms, in an e-mail exchange, Jean-Pierre Charras confirmed that he prefers "KiCad." He also reports that because of library issues, the Macintosh version is currently unofficially supported.

Other Packages

There are numerous options for schematic capture and P.C. board layout. Other software packages include gEDA 0, TinyCAD 0, and Eagle 0. The gEDA project is primarily for GNU/Linux; it has simulation tools and is described as a confederation rather than an integration of tools. TinyCAD is a simple schematic capture tool for use with Windows. I only briefly looked at XCircuit 0 and FreePCB 0. KiCad, gEDA, TinyCAD, XCircuit, and FreePCB are all free software.

Eagle is proprietary and includes schematic capture, P.C. board layout, and auto-routing software. The light edition can be used gratis but with restrictions. A schematic can only use one sheet of paper. Also, a layout can only have two copper layers and is limited to 4 by 3.2 inches in size. For a fee, however, there are numerous options available with the full edition.

Summary

KiCad is a useful package for producing schematics and P.C. board artwork. I find it particularly useful in my research and with my students, and others will also find it useful in these and other capacities. In particular, KiCad produces industry standard artwork. KiCad is GNU GPL licensed 0 and is an exceptional example of free software. I encourage you to consider using KiCad.

References

http://www.lis.inpg.fr/realise_au_lis/kicad/
http://www.geda.seul.org/
http://tinycad.sourceforge.net/
http://opencircuitdesign.com/xcircuit/
http://www.freepcb.com/
http://www.cadsoftusa.com/
http://www.gnu.org/licenses/licenses.html

Biographies

JONATHAN HILL is an assistant professor in Electrical and Computer Engineering at the University of Hartford in Connecticut. He instructs graduate and undergraduate computer engineering computer courses, directs graduate research, and performs research involving embedded microprocessor based systems. Specific projects involve digital communications, signal processing, and intelligent instrumentation.

BOOK REVIEW

CONTROL SYSTEM ENGINEERING

AUTHORED BY NORMAN NISE; WILEY, JOHN AND SONS, INC.; © 2007

Reviewed by Vijay Vaidyanathan, University of North Texas

Book Description

Control Systems Engineering, now in its *Fifth Edition*, takes a practical approach to control systems engineering. Presenting clear and complete explanations, the text shows the engineering student how to analyze and design feedback control systems that form a vital part of today's cutting edge technology. By continuing the same physical system in each chapter, the book's case studies provide a simple and realistic view of each stage of the control design process. The book also endeavors to present a combination of qualitative and quantitative explanations that provide insight into the design of parameters and system configurations. The book's highlight is its extensive practice in using MATLAB, Simulink, and the SISO Design Tool—industry standards that will serve the future engineer well.

Features

This book is targeted to meet the needs of electrical engineers and technicians who design and build hardware and software for control systems as well as senior-level students in Engineering Technology programs (electronic, biomedical, and computer engineering technologies) at technical colleges and junior-level students in traditional university engineering programs. Also appropriate for courses on instruction in government and industry.

Review

The clarity and flow of the material is fine and commensurate with the intended audience. This textbook is an extremely comfortable read. It covers a lot of material that is normally associated with classic control theory and other topics, including fundamentals of state space and digital control. The level of the book is suitable for its intended audience. The depth of coverage is lacking in the chapter on state space representations. The level of math in this chapter is appropriate taking into view the intended audience. The text is well organized and presents plenty of solved examples on various facets of control systems with clear formulae. However, the text assumes you have a background in the basic differential equations and Laplace transform.

The content presented in the book is correct and also current. However, currency of topics would be better with more detailed discussion of topics, as stated below:

1) State space representation
2) Digital control
3) LabVIEW applications for control systems

Assertions in the book are backed up with further information and clear examples. Addition of MATLAB codes after solved examples is an excellent idea. Also, solving application examples introduces students to the practical world of control systems.

The figures in the book are illustrative of the material presented. The number of figures is just right. All tables presented in this book are effective.

INSTRUCTIONS FOR AUTHORS MANUSCRIPT REQUIREMENTS

THE INTERNATIONAL JOURNAL OF MODERN ENGINEERING is an online and print publication, specifically for the Engineering, Engineering Technology, and Industrial Technology professionals. Submissions to this journal, such as an article submission, peer-review of submitted documents, requested editing changes, notification of acceptance or rejection, and final publication of the accepted manuscript will be handled electronically.

All manuscripts must be submitted electronically. Manuscripts submitted to the International Journal of Modern Engineering must be prepared in Microsoft Word 98 or higher (.doc) with all pictures, jpg's, gif's. pdf's included in the body of the paper. All communications must be conducted via e-mail to the manuscript editor at fattarzadeh@central.uh.edu and a copy must be sent to the editor at editor@ijme.us

The editorial stuff of the International Journal of Modern Engineering reserves the right to format any submitted word document in order to present submissions in an acceptance PDF format in the online journal. All submitted work content will not be changed without express written consent from the author(s).

1. Word Document Page Setup: Top = 1", Bottom = 1", Left=1.25", and Right = 1.25". This is the default setting for Microsoft Word. Do Not Use Headers or Footers

2. Text Justification: Submit all text as "LEFT JUSTIFIED" with No Paragraph Indentation.

3. Page Breaks: No page breaks are to be inserted in your document.

4. Font Style: Use 11-point Times New Roman throughout the paper except where indicated otherwise.

5. Image Resolution: Images should 96 dpi, and not larger than 460 X 345 Pixels.

6. Images: All images should be included in the body of the paper. (.jpg or .gif format preferred)

7. Paper Title: Center at the top with 18-point Times New Roman (Bold).

8. Author and Affiliation: Use 12-point Times New Roman. Leave one blank line between the Title and the "Author and Affiliation" section. List on consecutive lines: the Author's name and the Author's Affiliation. If there are two authors follow the above guidelines by adding one space below the first listed author and repeat the process. If there are more than two authors, add on line below the last listed author and repeat the same procedure. Do not create a table or text box and place the "Author and Affiliation" information horizontally.

9. Body of the Paper: Use 11-point Times New Roman. Leave one blank line between the "Author's Affiliation" section and the body of the paper. Use a one-column format with left justification. Please do not use space between paragraphs and use 0.5 indentation as break between paragraphs.

10. Abstracts: Abstracts are required. Use 11-point Times New Roman Italic. Limit abstracts to 250 words or less.

11. Headings: Headings are not required but can be included. Use 11-point Times New Roman (ALL CAPS AND BOLD). Leave one blank line between the heading and body of the paper.

12. Page Numbering: The pages should not be numbered.

13. Bibliographical Information: Leave one blank line between the body of the paper and the bibliographical information. The referencing preference is to list and number each reference when referring to them in the text (e.g. [2]), type the corresponding reference number inside of bracket [1]. Consider each citation as a separate paragraph, using a standard paragraph break between each citation. Do not use the End-Page Reference utility in Microsoft Word. You must manually place references in the body of the text. Use font size 11 Times New Roman.

14. Tables and Figures: Center all tables with the caption placed one space above the table and centered. Center all figures with the caption placed one space below the figure and centered.

15 Page limit: Submitted article should not be more than 15 page.

California State University
Northridge

The *Online* Master of Science in Engineering Management

Continue working full time while earning your online master's degree - **in just two years.** Our nationally recognized, fully accredited program, from CSUN's College of Engineering and Computer Science and The Tseng College, will give you the leadership skills and organizational tools to boost your career to the next level. And it will help you learn to handle the challenges of managing technical projects and personnel.

The Engineering Management program at Cal State Northridge offers technical professionals the opportunity to gain knowledge and skills pertinent to the entrepreneurial and intrapreneurial management of existing and emerging technologies. The flexible interdisciplinary curriculum stresses the development of technological decision-making capabilities, while enabling continued intellectual growth in selected discipline areas. In so doing, it meets the growing needs for competent technologists with relevant management expertise.

A System Designed for You

CSUN is a **recognized leader in distance learning** and we've applied all of our experience to make the Engineering Management Distance program first in its field. For example:

- We use state of the art technology that is powerful but easy to use
- Our leading-edge curriculum offers you both academic excellence and real-world relevance
- We provide a full range of student services to support your learning experience

Advance Your Career

Apply your new program principles to a diverse range of industries such as:

- Software Development
- Oil Industry
- Communications
- Medical Research
- Nanotechnology
- Aerospace
- Defense
- Manufacturing

Don't follow—Lead!

For more information, contact us today!

- Myriam Cedeno, Program Manager,
  Phone 818-677-7707
  Email: myriam.cedeno@csun.edu
- MSEM Program Director,
  Phone: 818-677-2167
  Email: msem@csun.edu or
  http://exlweb.csun.edu/em/

College of Engineering and Computer Science
The Tseng College

IJME NOW SEEKS SPONSORS

IJME IS NOW THE OFFICAL AND FLAGSHIP JOURNAL OF INTERNATIONAL ASSOCATION OF JOURNALS AND CONFERENCE (IAJC)
www.iajc.org

The International Journal of Modern Engineering (IJME) is a highly-selective (acceptance rate of 10-20%), peer-reviewed journal covering topics that appeal to a broad readership of various branches of engineering and related technologies. IJME is steered by IAJC distinguished board of directors and is supported by an international review board consisting of prominent individuals representing many well-known universities, colleges, and corporations in the United States and abroad.

IJME Contact Information

General questions or inquiry about sponsorship of the journal should be directed to:

Mark Rajai, Ph.D.
Editor-In-Chief
Office: (818) 677-2167
Email: editor@ijme.us
Department of Manufacturing Systems Engineering & Management
California State University-Northridge
18111 Nordhoff St.
Northridge, CA 91330